MODELLING THE IMPACT OF LANDUSE/LAND COVER CHANGE ON THE STREAM FLOW OF UPPER GUDER RIVER CATCHMENT USING SWAT, ABBAY BASIN, ETHIOPIA

MASTERS SCIENCE THESIS

TAKELE DUFERA TASGARA

HAWASSA UNIVERSITY, HAWASSA, ETHIOPIA

MARCH, 2021

MODELLING THE IMPACT OF LANDUSE/LAND COVER ON THE STREAM FLOW OF UPPER GUDER RIVER CATCHMENT USING SWAT, ABBAY BASIN, ETHIOPIA

TAKELE DUFERA TASGARA

A THESIS SUBMITTED TO THE
FACULTY OF BIO-SYSTEMS AND WATER RESOURCE ENGINEERING,
DEPARTMENT OF WATER RESOURCE AND IRRIGATION ENGINEERING
HAWASSA UNIVERSITY, INSTITUTE OF TECHNOLOGY
SCHOOL OF GRADUATE STUDIES
HAWASSA UNIVERSITY
HAWASSA, ETHIOPIA

IN PARTIAL FULFILLMENT OF
THE REQUIREMENTS FOR THE DEGREE OF
MASTERS OF SCIENCE IN WATER RESOURCE AND IRRIGATION ENGINEERING
(SPECIALIZATION: WATER RESOURCE ENGINEERING AND MANAGEMENT)

MARCH, 2021

Approval Page

As the thesis advisors, we here approve that, we have read and evaluated this thesis prepared by **Takele Dufera** entitled 'Modeling The Impact of Landuse/Land Cover Change on the Stream Flow of upper Guder River Catchment Using SWAT' submitted in partial fulfillment of the requirements for the degree of Master's with specialization in Water Resource Engineering and Management, the Graduate Program of the Faculty of Bio-systems and Water Resource Engineering, Department of Water Resource and Irrigation Engineering. Therefore we recommend that the student has fulfilled the requirements and hence hereby can submit the thesis to the department.

APPROVED BY:

Tewodros Assefa (Ph.D.)		_____
(Major Advisor)	Signature	Date
Nigatu Wondrade (Ph.D.)		_____
(Co-Advisor)	Signature	Date

Declaration

I, Takele Dufera, declare that this thesis, which I submit to the School of Graduate Studies of Hawassa University in partial fulfillment of the degree of Masters of Science in Water Resource Engineering and management, is my original work and that it has not been presented and will not be presented, in whole or in part, by me to any other University for similar or any other degree award. Additionally, I reasonably ensure that the work is original and to the best of my knowledge and has not been taken from other sources except where such works have been cited and acknowledged within the text.

Name: Takele Dufera Tasgara

Signature: _____

Acknowledgment

First of all, I would like to thank God for his never-ending love, care, and giving me the stamina to accomplish this research well in a given period. This day what God has done for me is really beyond what I can imagine and I have dreamt. Indeed, thanks for everything you have been doing for me.

My deep gratitude spirits to my major advisor Dr. Tewodros Assefa (Ph.D.) and my Co-Advisor Dr. Nigatu Wondrade(Ph.D.) for their continuous encouragement, advice, support and, valuable guidance throughout this study and, all their contribution through advising, materials support, and also trust and confidence makes me work on my interest topic.

I am very grateful to the ministry of education and Bule Hora University for sponsoring me and allowing me to take part in the Master Program at Hawassa University.

I am most grateful to my Father Dufera Tasgara for encouraging me from the beginning of my foundation, but my Father didn't saw this result, I want to say thanks and was great throughout my life. My heartfelt thanks to my Mom, my wife Beshatu Tabor, brothers and sisters whose love, sacrifice, and prayers kept me going during the last few years.

I would like to acknowledge the Ministry of Water, Irrigation, and Energy (MOWIE) particularly hydrology, GIS department, and the Ethiopian Meteorological Service Agency for providing me the relevant data and information required free of payment.

Lastly I thanks a lot to all my friends who also supported me through their friendship and professional help who stand with me through their contribution by appreciable ideas.

List of Acronyms and Abbreviations

ARS	Agricultural Research Service
CN	Curve Number
CSA	Central Statistical Agency
DEM	Digital Elevation Model
DMC	Double Mass Curve
DS	Standard Deviation
EROS	Earth Resources Observation and Science
ETM+	Enhanced Thematic Mapper Plus
FAO	Food and Agricultural Organization
FDRE	Federal Democratic Republic of Ethiopia
GIS	Geographic Information System
GLCF	Global Land Cover Facility
GLUE	Generalized Likelihood Uncertainty Estimation
GWQ	Ground Water Flow
HBV	Hydrologisika Bayraans Vattenbalans-avediling
HEC-HMS	Hydraulic Engineering Centre-Hydrologic Modeling System
HRU	Hydrological Response Unit
HWSD	Harmonized World Soil Database
IGBP	International Geo-sphere Biosphere Program
IHDP	International Human Dimension Program
ISODATA	Iterative Self-Organizing Data Analysis
LU/LC	Landuse/Land Cover
MCMC	Markov Chain Monte Carlo
MLC	Maximum Likelihood Classification
MOWIE	Ministry of Water, Irrigation and Energy
NMSAE	National Meteorological Service Agency of Ethiopia
NRCS	Natural Resources Conservation Service
NSE	Nash and Sutcliffe Coefficient of Efficiency
PBIS	Percent of Bias
R^2	Coefficient of Determination

RS	Remote Sensing
SCS	Soil Conservation Service
SRTM	Shuttle Radar Topographic Mission
SUFI2	Sequential Uncertainty Fitting two
SURQ	Surface Runoff
SWAT	Soil and Water Assessment Tool
SWAT_CUP	Soil and Water Assessment Tool, Calibration and Uncertainty Program
TM	Thematic Mapper
UNESCO	United Nations Educational, Scientific and Cultural Organization
USDA	United States Department of Agriculture
USGS	United States Geological Survey
UTM	Universal Traverse Mercator
WGEN	Weather Generator
WGS	World Geodetic System

Table of Contents

List of Tables

List of Figures

List of Tables in Appendices

List of Figures in Appendices

Abstract

Water resources are a critical component of any type of socio-economic development all over the world. Due to extensive agricultural practices, the LU/LC change was the cause of streamflow changes. The main objective of this research was to model the impact of landuse/land cover change on the streamflow of Upper Guder River Catchment using the SWAT model, by using meteorological data in the period between 1989 -2018. Upper Guder River Catchment was one of the catchment of the headwaters in the south Abbay Basin. In this study, the impact of LU/LC change *was carried out by using the Soil Water Assessment Tool (SWAT2012) model, which was integrated with GIS10.3 software. GIS and ERDAS IMAGINE2014 were used to generate landuse/land cover maps from Landsat TM, TM, and ETM+ acquired in the years 1989, 2002, and 2018 respectively. The land cover maps were generated using the maximum likelihood algorithm of supervised classification. The classified maps were assessed using confusion metrics. The results of the analysis showed that the Agricultural land has expanded during the study period of 1989-2018. During the study period, forest land, and shrub and grassland decreased by 6.48% and 4.23% respectively while Agricultural land and Built-up area increased by 8.04% and 2.69% respectively. Using three land cover maps, three SWAT model setup were run to evaluate the impacts of landuse/land cover changes on the streamflow of the study catchment. The performance of the SWAT model was evaluated through sensitivity analysis, calibration, and validation by using SWAT-CUP. Statistical measures like coefficients of determination and Nash–Sutcliffe were used to evaluate the model and it resulted in 0.84 and 0.74 for calibration and 0.83 and 0.72 for validation respectively. During the study periods, the simulation result indicated that streamflow increased in the wet season and short rainy season streamflow by 10.04% and 5.25% respectively, while decreasing by 6.60% in the dry season. The Surface Flow (SURQ) increased by 5.73% while Groundwater Flow (GWQ) decreased by 2.26% due to the increment of Agricultural land. The model results showed that the streamflow characteristics changed due to the landuse/land cover changes during the study period. The catchment was sensitive to past LU/LC change, so it needs an effective integrated participatory approach for catchment management.*

Keywords: SWAT Model, Upper Guder River Catchment, Landuse/land cover change, Streamflow

1. INTRODUCTION

1.1. Background

Nowadays water resources are a critical component for any type of socio-economic development all over the world. Thus, its availability and use have to be at the center of any discussion of development. Deterioration of the global freshwater resources becomes the forefront of scientific and political agenda concerning global environmental changes in landuse and bio-diversity (Montoya and Raffaelli, 2010; Miranda et al., 2011). Landuse land cover change has become a serious environmental concern at the global, regional, and local scales (Mishra et al., 2014; Zhan et al., 2014 and Kumar et al., 2015). Changes in landuse/land cover play important roles in global environmental change because the changes have affected the sustainability, biodiversity, and interactions between the earth and atmosphere (Zhan et al., 2014 and Kumar et al., 2015).

Landuse/land cover change has been also challenging in Ethiopia. At the beginning of the 19th century, 40% of land in the country was covered by forests (Abebe, 2005; Mengistie et al., 2013 and Birhanu, 2014). However, a rapid rate of deforestation and land degradation led to a loss of plant and animal species (Kaimowitz and Angelsen, 1998). Ethiopia has a population of more than 100 million with a growth rate of 2.7%, of this about 80% of the population solely depends on agricultural practices as a source of employment and income (CSA, 2015). The increase of population density leads to clear-cutting, shrinking forests and grasslands, the expansion of cultivated areas, and intensified landuse resulting in almost complete abandonment of the fallow systems (Hurni et al., 2005).

Ethiopia has twelve river basin, from those Abbay River Basin was a significant part of Ethiopia, covering an area of 199,812 km^2. Due to extensive agricultural practices, Landuse/land cover change was the main cause of soil degradation and could significantly change the streamflow availability (Tolba et al., 1992). Studies in a different part of the Abbay basin revealed that there were many factors which caused LU/LC changes among which population density was one of the major factors which further has caused change on streamflow (Haregeweyn et al., 2015).

Quantifying the effects of landuse change on streamflow has recently been given much attention by the scientific communities (e.g. Jiang et al., 2011; Yang et al., 2012). Landuse change was caused by multiple interacting factors of the coupled human and environment systems (Lambin,

2003). This was attributed to different anthropogenic activities, e.g. intensive land cultivation, deforestation, overgrazing, urbanization, afforestation, and reforestation. The heterogeneity of topography, land use, soil, and geology, on the one hand, and limitation of hydro-meteorological data on the other hand is considered to be the major scientific challenges often preclude to study landuse change impact on hydrology (DeFries and Eshleman, 2004). The underlying mechanisms, which underpin the impact of landuse change on streamflow was not yet fully understood (Wang et al., 2007b).

In Ethiopia, Rientjes et al., (2011b) showed that the LU/LC change was the cause of streamflow changes. Most recently, Kidane et al., (2018) reported a decrease of the dry season flows, attributed to the clearance of natural vegetation cover and increased agricultural expansion. Studying on the Upper Guder River Catchment under the impact of landuse/land cover change was particularly very important in improving water management efficiency and benefiting various water use needs such as irrigation and small scale hydropower and also it might be used for recreation, and environmental protection. Besides the mentioned purposes, highly it would be used for better management and planning of rivers. Gathering historical patterns of change and modeling helps for a better understanding of processes of change that helps to improve a land management practice (Aithal et al., 2013; Pontius and Chen, 2006 and Behailu, 2010).

Based on the process description, the SWAT model has been more efficient than other models (Sith and Nadaoka, 2017; Polanco et al., 2017). SWAT is a well-developed tool for analyzing the effects of water resource practices in the most challenging watersheds. Therefore, the SWAT model was the best modeling of a semi-distributed physical-based simulation model. The interface of the SWAT model was compatible with a GIS that can integrate numerous available geospatial data (Neitsch et al., 2005).

1.2. Statement of the Problem

The relationship between land and water was the interest of worldwide. The change in landuse emanating from expanding the agricultural land in Ethiopia needs primary concern (FDRE, 2004). Lack of proper landuse plan and management practices that could increase agricultural products with limited land and economic resource. This was further affecting the water resource of the country (Teferi et al., 2010; Hadgu, 2008).

The LU/LC change has a significant impact on natural resources. However, to model the impact of LU/LC change on streamflow, it is important to have an understanding of the past LU/LC change and the hydrological processes of the catchments. Understanding the types and impact of LU/LC change was an essential indicator for water resource base analysis and development of effective and appropriate response strategies for sustainable management of natural resources in the country in general and particularly in the study area.

In Upper Guder River Catchment nonetheless research was done concerning the impact of landuse/land cover on streamflow in particular attention. Therefore, this research was initiating to minimize the adverse impact of LU/LC change at the headstream of the catchment. The importance of streamflow for the sustainable development of water resource and LU/LC change on catchment were not yet well understood. Therefore, it was necessitated to give more attention to LU/LC and streamflow. Hence SWAT model was selected because of their structure was more physically-based, and they are less demanding on input data than fully distributed models and can evaluate the impact of landuse change in the catchment with varying soils, landuse and management conditions over the long periods, and primarily as a strategic planning tool (Neitsch et al., 2005).

The overall objective of this study was to model the streamflow of the Upper Guder River Catchment under the impact of LU/LC change using the SWAT model. This study provides important information that decision-makers would be needed to assist with water resources management in the Upper Guder River Catchment under changing LU/LC conditions.

1.3. Objectives of the Study

1.3.1. General Objective

The general objective of this study was to model the streamflow of the Upper Guder River Catchment under the impact of LU/LC change using the SWAT model.

1.3.2. Specific Objectives

The followings were the specific objectives of this study:

1. To determine the landuse/land cover change in the catchment for the last three decades (1989-2018) using Landsat images and RS software packages.
2. To evaluate the performance of the SWAT model for the study catchment in the period between 1989 -2018.
3. To evaluate the effects of landuse/land cover change on the streamflow of the catchment for the years 1989, 2002, and 2018 using the SWAT model.

1.4. Research Questions

The research questions addressed in this study were:

1. What magnitude of landuse/land cover change has occurred in the Upper Guder River Catchment for the time range between1989-2018?
2. Can the SWAT model show the required performance for the catchment using estimated LU/LC change?
3. What are the effects of landuse/land cover change on the streamflow of the catchment for the year of 1989, 2002, and 2018?

1.5. Significance of the Study

This research finding measures for the knowledge of how the landuse/land cover change effects on stream flow of the catchment. The knowledge how landuse/land cover changes influences catchment properties and the compressive analysis of the catchment will enables to local governments, farmers and policy makers about proper land use and different management options. The findings of this research used to make the stakeholders an effective integrate participatory to take action on the protection of catchment management.

In addition, this study is expectable to help concerned bodies in planning, developing and managing water resource projects in the study area and be an input for those who are interested to further research in related field and area of study.

1.6. Scope of the Study

The time period considered in the study was from 1989-2018 whereas the spatial range of the study was in the Abbay Basin in particular at the Upper Guder River Catchment which covers 2290Km^2. Moreover, the study quantifies the impact of LU/LC change and evaluate the LU/LC change on the hydrological regime, especially on streamflow. Based on the available data, the types and impact of LU/LC change will be an indicator for resource base analysis and development of effective and appropriate response strategies for sustainable management of natural resources for the study area. So by using this, the study simulate for adverse impacts. This would be achieved through a method that combines the hydrological model (SWAT) to simulate the hydrological processes.

The impact of Landuse/land cover on streamflow was not analyzed in particular rather different landuse/land cover and climate scenarios developed based on previous studies conducted in the Abbay Basin of the central highland of Ethiopia.

2. LITERATURE REVIEW

2.1. Definition and Concepts of Landuse/Land Cover Changes

The definition of landuse is physical and biophysical characteristics or state of Earth's surface which way establishes a direct link between land cover and the actions of people in their environment (FAO and MoWIE, 2013). Factors driving LU/LC change include an increase in the human population and population response to economic opportunities (Lambin et al., 2000).

According to Meyer and Turner (1994), Landuse/Land Cover Changes (LU/LC change) is the shift in intent and/or management constitutes landuse/land cover. Deforestation and forest degradation have been influenced by a combination of underlying driving forces, including unclear land tenure, population growth, market (wood extraction), and sociopolitical factors (Bekele, 2003; Dessie and Christianson, 2008), that different type of landuse/land cover has an impact to increase or decrease streamflow. Crops need less soil moisture than forests; therefore, the rainfall satisfies the shortage of soil moisture in agricultural lands more quickly than in forests thereby generating more runoff when the area under agricultural land is extensive. Hence, this leads to increases in streamflow.

The landuse/land cover change assessment is an important step in planning sustainable land management that can help to minimize agro-biodiversity losses and land degradation, especially in developing countries like Ethiopia (Tolessa et al., 2016). According to the International Geo-sphere Biosphere Program and The International Human Dimension Program (IGBP-IHDP) (1999), land cover refers to the physical and biophysical cover over the surface of the earth, including distribution of vegetation, water, bare soil, and artificial structures. Landuse refers to the intended use or management of the land cover type by human beings such as agriculture, forestry, and building construction. Landuse/land cover change is commonly grouped into two broad categories conversion and modification (Meyer and Turner, 1994).

I. Conversion refers to a change from one cover or use category to another (e.g. from forest to grassland).
II. Modification, on the other hand, represents a change within one landuse/land cover category (e.g. from rainfed cultivated area to irrigated cultivated area) due to changes in its physical or functional attributes. These changes in landuse/land cover systems have important environmental consequences through their impacts on soil and water, biodiversity, and microclimate (Lambin, 2003).

There is a significant statistical correlation between population growth and land cover conversion in most African, Asian, and Latin American countries (Meyer and Turner, 1994). Due to the increasing demands of food production, agricultural lands are expanding at the expense of natural vegetation and grasslands (Lambin, 2003). In most developing countries like Ethiopia, population growth has been a dominant cause of landuse/land cover change than other forces (Sage, 1994).

2.1.1. Drivers of Landuse/Land Cover Change

In the past two centuries, the impact of human activities on land has grown enormously because of population increase, technological development, and the requirements thereafter, altering entire landscapes, and ultimately impacting the biodiversity, nutrient, and hydrological cycles (Sherbinin, 2002), especially in the developing countries. The driving forces to land cover are activity could be technological and demographic (Gashaw et al., 2018). Hence, Landuse/Land Cover dynamics is a result of complex interactions between several biophysical conditions which may occur at various temporal and spatial scales (Sherbinin, 2002).

The local human activities expressing the drivers can be determined by measuring the rates and types of changes and analyzing other relevant sources of data like demographic profiles, household characteristics, and policies related to land resources administration (Oumer, 2009). Stream and river control works may have a serious local influence on channel erosion. Channel straightening which increases slope and flows velocity may initiate channel and bank erosion (Julien, 2010). If the bed of the mainstream is lowered, the beds of tributary streams are also lowered. In many instances, such bed degradation is beneficial because it restores the flood-carrying capacity of channels (Julien, 2010).

SWAT models have been used to predict the impact of landuse change on environmental cycles. Although their solutions vary in terms of the effect magnitude, most of them show that landuse change can be an important variable in SWAT models as well as they state that SWAT would be a useful tool for further investigation of landuse dynamic implementation (Friedrich et al., 2012)

2.2. Image Classification

A landuse/land cover classification system which can effectively employ orbital and high- altitude remote sensor data should meet the following criteria (Anderson et al., 1976):

1. The minimum level of accuracy in the identification of landuse/land cover categories from remote sensor data should be at least 85 percent.
2. The accuracy of interpretation for the several categories should be about equal.
3. Repeatable or repetitive results should be obtainable from one interpreter to another and from one time of sensing to another.
4. The classification system should be applicable over extensive areas.
5. The categorization should permit vegetation and other types of land cover.
6. The classification system should be suitable for use with remote sensor data obtained at different times of the year.
7. Effective use of subcategories that can be obtained from ground surveys or the use of a larger scale or enhanced remote sensor data should be possible.
8. Aggregation of categories must be possible.
9. A comparison with future landuse data should be possible.
10. Multiple uses of land should be recognized when possible.

2.3. Hydrological Models

Hydrological models are mathematical descriptions of components of the hydrological cycle (Cunderlik, 2003). However, hydrological models are in general designed to meet one of the two primary objectives (Matjaz and Marina, 2012). The one objective of the watershed hydrologic modeling is to get a better understanding of the hydrologic processes in watersheds. The other objective is for studying the potential impacts of changes in landuse/land cover. Based on the process description, the hydrological models can be classified into three main categories (Cunderlik, 2003).

- ✓ **Lumped models:** Parameters of lumped hydrologic models do not vary spatially within the basin and thus, basin response is evaluated only at an outlet, without explicitly accounting for the response of individual sub-basins. The parameters often do not represent the physical features of hydrologic processes and usually involve a certain degree of empiricism. These models are not usually applicable to event-scale processes. If the interest is primarily in the discharge prediction only, then these models can provide just as good simulations as complex physical-based models (Fekadu et al., 2005), (Uttam et al., 2020), and (Velazquez et al., 2010).

- ✓ **Distributed models:** Parameters of distributed models are fully allowed to vary in space at the resolution usually chosen by the user. The distributed modeling approach attempts to incorporate data concerning the spatial distribution of parameter variations together with computational algorithms to evaluate the influence of this distribution on simulated precipitation-runoff behavior. Distributed models generally require a large amount of (often unavailable) data. However, the governing physical processes are modeled in detail, and if properly applied, they can provide the highest degree of accuracy (Abbott et al., 1986), (Refsgaard, 1996).
- ✓ **Semi-distributed models:** Parameters of semi-distributed (simplified distributed) models are partially allowed to vary in space by dividing the basin into several smaller sub-basins. The main advantage of these models is that their structure is more physically-based than the structure of lumped models, and they are less demanding on input data than fully distributed models. SWAT (Arnold et al., 2012), HEC-HMS (ACE, 2001), and HBV (Bergstrom, 1995), are considered as semi-distributed models.

Hydrologic models can be further divided into event-driven models, continuous processes models, or models capable of simulating both short-term and continuous events (Matjaz and Marina, 2012). Event-driven models are designed to simulate individual precipitation-runoff events. Their emphasis is placed on infiltration and surface runoff. Typically, event models have no provision for moisture recovery between storm events and, therefore, are not suited for the simulation of dry weather flows. On the other hand, continuous process models simulate instead of a longer period, predicting watershed response both during and between precipitation events. They are suited for simulation of daily, monthly, or seasonal streamflow, usually for long-term runoff volume forecasting and for estimating of water yield (Cunderlik, 2003).

2.3.1. Hydrological Model Selection Criteria

Various criteria can be used for choosing the right hydrological model for a specific problem. These criteria's are always project dependent, every project has its specific requirements and needs. Further, some criteria are user-dependent (and therefore subjective). Among the various project-dependent selection criteria there are common, fundamental that must be always answered (Cunderlik, 2003). Choosing the most appropriate model for simulating the hydrological flows in a particular watershed and the specific climate was consistently a major part of the global modeling

process. For example, the SWAT model has been more efficient than other models (Sith and Nadaoka, 2017; Polanco et al., 2017).

SWAT is a well-developed tool for analyzing the effects of water resource practices in the most challenging watersheds. Researchers used the SWAT model for hydrological modeling and water resource practices in diverse climate and terrain features (Panhalkar, 2014; Costa et al., 2015; Tuppad et al., 2011, Mankin, L. and Haron et al., 2016). The SWAT model simulates various water functions such as filtration, evapotranspiration, runoff water production, underground recharge, other processes such as watershed growth, vegetation and crops, nitrate, and phosphorus progress, and surface waters (Jha, 2011; Khatun, 2018).

2.3.2. Description of the SWAT model

The SWAT model is one of the models developed at the USDA-ARS (Arnold, 1998) during the early 1970s. The SWAT model is a semi-distributed physical-based simulation model and can predict the impacts of landuse change and management practices on hydrological regimes in watersheds with varying soils, landuse and management conditions over the long periods and primarily as a strategic planning tool (Neitsch, 2005).

Soil and Water Assessment Tool (SWAT) is a physically-based, continuous-time, and computationally efficient hydrological/water quality model, which uses readily available inputs (Essenfelder, 2016). As a physically-based model, SWAT uses hydrologic response units (HRUs) to describe spatial heterogeneity in terms of land cover, soil type, and slope within the watershed (Arnold et al., 2012).

The SWAT system is embedded within a Geographic Information System (GIS) that can integrate various spatial environmental data including soil, land cover, climate, and topographic features (Arnold et al., 2012). It was developed to predict the impact of land management practices on water, sediment, and agricultural chemical yields in large complex watersheds with varying soils, landuse and management conditions (Neitsch et al., 2005). It enables users to study long term impacts and hence is being used extensively in the U.S. and other parts of the world to assess the impact of global climate change and water quality (Neitsch et al., 2005).

There are two scale levels of subdivision; the first is that the watershed is divided into several sub-watersheds based upon drainage areas of the attributes, and the other one is that each sub-watershed

is further divided into several hydrological response units (HRUs) based on landuse/land cover, soil and slope characteristics (Arnold et al., 2012). The SWAT model simulates eight major components: hydrology, weather, sedimentation, soil temperature, crop growth, nutrients, pesticides, and agricultural management (Neitsch, 2005). Major hydrologic processes that can be simulated by the model include Evapotranspiration, surface runoff, infiltration, percolation, shallow aquifer, and deep aquifer flow, and channel routing (Neitsch et al., 2005)**.** Streamflow was determined by its components (surface runoff and the groundwater flow from shallow aquifer).

SWAT splits hydrological simulations of a watershed in two major phases; the land phases and routing phases. The land phases of the hydrological cycle control the amount of water, sediment, nutrient, and pesticide loadings to the main channel in each sub-basin. While the routing phases consider the movement of water, sediment, and agricultural chemicals through the channel network to the watershed outlet (Ma X, 2009). The land phases of the hydrological cycle is modeled in SWAT based on the water balance equation (Neitsch, 2005).

$$Swt = Swo + \sum_{i=1}^{t}(Rday - Qsurf - Ea - Wseep - Qgw) \quad \text{.....2.1}$$

Where:-

Swt: soil water content (mm)

SWo: initial water content (mm)

t: time in (days)

Rday: the amount of precipitation on the day i (mm)

Qsurf: the amount of surface runoff on the day i (mm)

Ea: the amount of Evapotranspiration on the day i (mm)

Wseep: the amount of water entering the vadose zone from the day i(mm), and

Qgw: the amount of return flow on the day i (mm)

For the complete model description, one may refer to SWAT theoretical documentation (Neitsch, 2005).

2.3.2.1. Surface Runoff

Surface runoff refers to the portion of rainwater that is not lost to interception, infiltration, and Evapotranspiration (Solomon, 2005). Surface runoff occurs whenever the rate of precipitation exceeds the rate of infiltration. SWAT offers two methods to estimate the surface runoff: the soil conservation service (SCS) curve number method (SCS, 1972) or the Green and Ampt infiltration

method (Green and Ampt, 1911). The Green and Ampt method needs sub-daily time step rainfall which made it difficult to be used due to the unavailability of sub-daily time step rainfall data. Therefore, the SCS curve number method was adopted.

The general equation for the SCS curve number method is expressed equation (2.2).

$$\mathbf{Qsurf} = \frac{(\mathbf{Rday}-\mathbf{Ia})^2}{(\mathbf{Rday}-\mathbf{Ia}+\mathbf{S})} \quad \text{.....2.2}$$

Where:-

Qsurf is the accumulated runoff or rainfall excess (mm),

Rday is the rainfall depth for the day (mm water),

Ia is an initial abstraction which includes surface storage, interception, and infiltration before runoff (mm water),

S is the retention parameter (mm water).

The retention parameter varies spatially due to changes with land surface features such as landuse, slope, and management practices. This parameter can also be affected temporal due to changes in soil water content. It is mathematically expressed as:-

$$S = 25.4 * \left(\frac{\mathbf{1000}}{\mathbf{CN}}\right) - 10) \quad \text{.....2.3}$$

Where CN is the curve number for the day its value is the function of landuse soil permeability and soil hydrologic group.

The initial abstraction, Ia, is commonly approximated as 0.2S, and equation (2.2) becomes:

$$Qsurf = \frac{(\mathbf{Rday}-\mathbf{0.2s})^2}{(\mathbf{Rday}+\mathbf{0.8s})} \quad \text{.....2.4}$$

SWAT includes two methods for calculating the retention parameter; the first one is retention parameter varies with soil profile water content and the second method is the retention parameter varies with accumulated plant Evapotranspiration. The soil moisture calculation method overestimates runoff in shallow soil. However, calculating daily CN as a function of plant Evapotranspiration, the value is less dependent on soil storage and more dependent on antecedent climate.

$$S = S_{max} * \left(1 - \frac{Sw}{(sw + \exp(w1 - w2 * sw))}\right) \quad \text{.....2.5}$$

Where S is the retention parameter for a given day (mm), S_{max} is the maximum value the retention parameter can achieve on any given day (mm), SW is the soil water content of the entire profile

excluding the amount of water held in the profile at wilting point (mm), and w1 and w2 are shape coefficients. The maximum retention parameter value, S_{max} is calculated by solving equation 2.3 using CN1

$$S_{max} = 25.4(\frac{1000}{CN1} - 10)\text{……..2.6}$$

When the retention parameter varies with plant Evapotranspiration, the following equation is used to update the retention parameter at the end of every day

$$S = S_{prev} + E_o * \exp\left(\frac{-cncoef - S_{prev}}{S_{max}}\right) - R_{day} - Q_{surf}\text{…….2.7}$$

Where S is the retention parameter for a given day (mm), S_{prev} is the retention parameter for the previous day (mm), E_o is potential Evapotranspiration for the day (mm per day), cncoef is the weighting coefficient used to calculate the retention coefficient for daily curve number calculations dependent on plant Evapotranspiration, S_{max} is the maximum value the retention parameter can achieve on any given day (mm), Rday is the rainfall depth for the day (mm) and Q_{surf} is the surface runoff (mm). The initial value of the retention parameter is defined as $S=0.9*S_{max}$.

The SCS curve number is a function of the soil permeability, landuse, and antecedent soil water condition. SCS defines three antecedent moisture conditions: I dry (wilting point), II average moisture, and III wets (field Capacity). The moisture condition I curve number is the lowest value the daily curve number can assume in dry conditions. The curve number for moisture conditions III and I are calculated with equations 2.8 and 2.9 respectively.

$$CN_1 = CN_2 - \frac{20*(100-CN_2)}{(100-CN_2+\exp(2.533-0.0636*(100-CN_2)))}\text{…….2.8}$$

$$CN_3 = CN_2 * \exp(0.00673 * (100 - CN_2)\text{…….2.9}$$

Where CN1 is the moisture condition I curve number, CN2 is the moisture condition II curve number and CN3 is the moisture condition III curve number.

For the definition of hydrological groups, the model uses the U.S. Natural resources conservation service (NRCS) classification. The classification defines a hydrological model group as a group of soils having similar runoff potential under similar storm and land cover conditions. Thus, soils are classified into four hydrological groups (A,B, C, and D) based on infiltration which represents high, moderate, slow, and very slow infiltration rates, respectively.

2.3.2.2. Ground Water Flow

To simulate the groundwater, SWAT partitions groundwater into two aquifer systems: a shallow, unconfined aquifer that contributes return flow to stream within the watershed and a deep, confined aquifer which contributes return flow to streams outside the watershed (Arnold et al., 2012). In SWAT the water balance for a shallow aquifer is calculated with equation (2.10).

$$aqshi = aqshi_{-1} + W_{rchrg} - Q_{gw} - W_{revap} - W_{deep} - W_{pumpsh} \quad \text{……..2.10}$$

Where:-

aqshi is the amount of water stored in the shallow aquifer on a day I (mm),

Aqsh i-1 is the amount of water stored in the shallow aquifer on day i-1(mm),

W rchrg is the amount of recharge entering the aquifer on a day I (mm),

Qgw is the groundwater flow, or base flow, or return flow, into the main channel on a day I (mm)

Wrevap is the amount of water moving into the soil zone in response to water deficiencies on a day I (mm),

Wdeep is the amount of water percolating from the shallow aquifer into the deep aquifer on day I (mm), and

Wpumpsh is the amount of water removed from the shallow aquifer by pumping on a day I (mm).

2.3.2.3. Flow Routing Phase

The second component of the simulation of the hydrology of watershed is the routing phase of the hydrological cycle. It consists of the movement of water, sediment, and other constituents (E.g. nutrients, pesticides) in the stream network. Two options are available to route the flow in the channel network: the available storage and Muskingum methods.

The available storage method uses a simple continuity equation in routing the storage volume, whereas the Muskingum routing method models the storage volume in channel length as a combination of wedge and prism storages. In the latter method, when a flood wave advances in to reach segment, inflow exceeds outflow, and wedge storage is produced. As a flood wave recedes or withdrawals, outflow exceeds inflow in the reach segment and a negative wedge is produced. In addition to the wedge storage, the reach segment contains a prism of storage formed by a volume of the constant cross-section along the reach length. The available storage method was used for

this study. The method was developed by (Williams, 1981). The equation of the available storage routing is given by:

$\Delta Vstored = Vin - Vout$ 2.11

Where:-

ΔV stored: a change in the volume of storage during the time step (m^3 water)

Vin: the volume of inflow during the time step (m^3 water), and

$Vout$: is the volume of outflow during the time step (m^3 water)

2.3.3. Evaluation of Model Performances

According to Arnold et al., (2012) the calibration and validation model performances can be assessed using three model evaluation criteria, Nash and Sutcliffe Coefficient of Efficiency (NSE), Coefficient of Determination (R^2), and Percent of Bias (PBIAS). Model evaluation was an essential measure to verify the robustness of the model.

The determination coefficient (R^2) describes the proportion of the variance in measured data by the model (Arnold et al., 2012). It was the magnitude linear relationship between the observed and the simulated values. R^2 ranges from 0 (which indicates the model is poor) to 1 (which indicates the model is very good), with higher values indicating less error variance, and the flow calibration procedure made by SWAT developers in Santhi, (2001) and Neitsch et al., (2005) was carefully followed. SWAT developers assumed an acceptable calibration for hydrology $R^2 > 0.6$ (Arnold et al., 2012).

The R^2 was calculated using the following equation:

$$\mathbf{R^2} = \frac{\sum_{\mathbf{i=1}}^{\mathbf{n}}[(\mathbf{Qi}-\mathbf{Qav})*(\mathbf{Pi}-\mathbf{Pav})]^{\mathbf{2}}}{\sum_{\boldsymbol{i=1}}^{\boldsymbol{n}}(\mathbf{Qi}-\mathbf{Qav})^{\mathbf{2}}*\sum_{\boldsymbol{i=1}}^{\boldsymbol{n}}(\boldsymbol{P}\mathbf{i}-\mathbf{Pav})^{\mathbf{2}}} \quad \text{..... 2.12}$$

Where:-

Qi: measured value

Pi: simulated value and

Qav: average observed value

Pav: average simulated value

The Nash and Sutcliffe Coefficient of efficiency (NSE) describes the deviation from the unit of the ratio of the square of the difference between the observed and simulated values and the variance

of the observations. The value of the coefficients varies from minus infinity to one with the latter value indicating perfect agreement between the simulated and observed data. A smaller NSE value indicates a poorer fit between the simulated and observed data

NSE was recommended and widely used in literature (Moriasi, 2007) therefore there is a lot of reported values for use as evaluation guidelines. NSE, in a simplified explanation by (Moriasi, 2007) is an indication of how well the plot of observed versus simulated data fits the 1:1 line and NSE > 0.5 (Santhi, 2001; Moriasi, 2007).

NSE was computed as shown in the following equation.

$$ENS = 1 - \frac{\sum_{i=1}^{n}(Qi-Pi)^2}{\sum_{i=1}^{n}(Qi-Qav)^2} \quad \text{.....2.13}$$

Where:-

Qi: measured value

Pi: simulated value and

Qav: average observed value

The percent bias (PBIS) describes the tendency of the simulated data to be greater or smaller than observed data, expressed as a percentage. Positive values indicate a tendency of the model to underestimate while negative values are indicative of overestimation. This test is recommended due to its ability to reveal any poor performance of the model (Moriasi, 2007).

$$\text{PBIAS} = \frac{\sum_{i}^{n}(\text{Qm}-\text{Qs})}{\sum_{i}^{n}\text{Qm}} * 100 \quad \text{.....2.14}$$

Where: Qm measured value and Qs is simulated

The evaluation was performed by visual and statistical comparison of the measured and simulated data. The graphical method provided an initial overview. The statistical criteria were used to evaluate the performance of the model.

2.3.4. SWAT Model Application in Ethiopia

The SWAT model application was calibrated and validated in some parts of Ethiopia, frequently in the Abbay Basin. The modeling of Didessa Watershed (in Abbay Basin) (Minichil, 2016) indicated that streamflow and sediment yield simulated with SWAT were reasonably accurate. The same study conducted on similar long term data can be generated from ungauged watershed using the SWAT model and modeling of Lake Tana Basin with SWAT also showed that the SWAT model was successfully calibrated and validated (Setegn, 2008). This study reported that the model

can produce reliable estimates of streamflow and sediment yield from complex watersheds. Rabo (2018) used the SWAT model performed to simulate runoff under the impact of past landuse/land cover and climate change of the Anger Sub-basin. According to this study, the SWAT model performed well in the simulation of runoff to Anger Sub-basin. The study further put that the model proved to be useful in capturing the process of streamflow.

In addition to the above, the SWAT model was tested for prediction of sediment yield in Anjeni gauged watershed by (Setegn, 2008). The study found that the observed values showed a good agreement at Nash-Sutcliff efficiency (NSE) of 80%. In light of this, the study suggested that the SWAT model can be used for further analysis of different management scenarios that could help different stakeholders to plan and implement appropriate soil and water conservation strategies. The SWAT model showed a good match between measured and simulated flow and sediment yield in Gumara watershed both in calibration and validation periods (Asres and Awulachew, 2010). Tekle, (2010) through modeling of Bilate watershed also indicated that the SWAT model was able to simulate streamflow at a reasonable accuracy. The literature reviewed and presented above showed that SWAT is capable of simulating hydrological and soil erosion process with reasonable accuracy and can be applied to the large and complex watershed.

2.4. Effects of Landuse/Land Cover on Stream Flow

Landuse/land cover change is one of the major challenges that affect the natural landscape. It is one of the main driving forces of global environmental change, and central to the sustainable development debate (Lambin et al., 2000). The present understanding of landuse effects on streamflow is derived from controlled experiments and manipulations of the land surface coupled with observations of hydrological processes, commonly precipitation inputs, and stream discharge outputs (DeFries and Eshleman, 2004).

According to Calder (1999), the largest changes in terms of land area, and arguably also in terms of hydrological impacts, reasonable from afforestation to deforestation activities. One of the direct effects of landuse changes on streamflow and hence on water resources is through its link with the evapotranspiration regime (Kidane et al., 2018). Any change in landuse and vegetation cover can have impacts on potential and actual evapotranspiration as well as on the discharge regime, which reflects the integrated behavior of all the hydrological processes acting in the catchment (Kidane et al., 2018).

2.5. Landuse/Land Cover Change Studies in Ethiopia

In Ethiopia, the land is used to grow crops, trees, animals for food, as building sites for houses and roads, or recreational purposes (Solomon et al., 2014). Most of the land in the country is being used by smallholders who cultivate the land for subsistence (Dessie and Christianson, 2008). With the rapid population growth and in the absence of agricultural intensification, smallholders require more land to grow crops and earn a living; it results in deforestation and landuse conversions from other types of land cover to cropland (Comenetz and Caviedes, 2002).

The researches that have been conducted in different parts of Ethiopia have shown that there were considerable landuse/land cover changes in the country. Most of these studies indicated that croplands have expanded at the expense of natural vegetation including forests and shrub lands; for example, (Abebe, 2005), Landuse/Land cover Change in the headstream of Abbay watershed in the northern part of Ethiopia (Kidane et al., 2018), Evaluating the impacts of climate and land use/land cover dynamics on the Hydrological Responses of the Upper Blue Nile in the Central Highlands of Ethiopia. Implications of Land use and land cover dynamics for mountain resource degradation in the northwestern Ethiopia (Zeleke, 2001). Kassa, (2009) Watershed Hydrological Responses to Changes in Land Use and Land Cover, and Management Practices at Hare Watershed. The changes of landuse/land cover that occurred in Yerer Mountain and its surroundings resulted in the expansion of cultivated land at the expense of the grasslands (Gebrehiwet, 2004, and Hadgu, 2008). They identified the decrease of natural vegetation and the expansion of agricultural land over 41 years in Tigray, the northern part of Ethiopia. They concluded that population pressure was an important driver for the expansion and intensification of agricultural land in recent periods.

To understand how LU/LC affects and interacts with global earth systems, information is Needed on what changes occur, where and when they occur, the rates at which they occur, and the social and physical forces that drive those changes (Solomon, 2005). Human impact on global land cover change, especially in terms of change from forest cover to other land covers, has been one of the important issues on global change research (Dessie and Christianson, 2008). In primitive times when there were little human population and low level of economic activity, deforestation was not a problem because the natural regeneration of forest was adequate to cover for any loss of forest by the human beings (Solomon et al., 2014).

3. MATERIALS AND METHODS

3.1. Description of the Study Area

3.1.1. Location

This study was conducted in the Upper Guder River Catchment. Upper Guder River Catchment was located in the central highlands of Ethiopia and has a drainage area of about 2290 square kilometers (Figure 3.1). It was one of the headwater catchment in the south Abbay Basin. The Upper Guder River Catchment extends between Latitude: 08°42'N to 09°10'N and Longitude: 37°25'E to 38º05’E and it was part of Abbay Basin. The Upper Guder River catchment borders with the Muger catchment to the east, the Awash Basin to the south, the Fincha catchment to the west, and the north by downstream of Guder catchment.

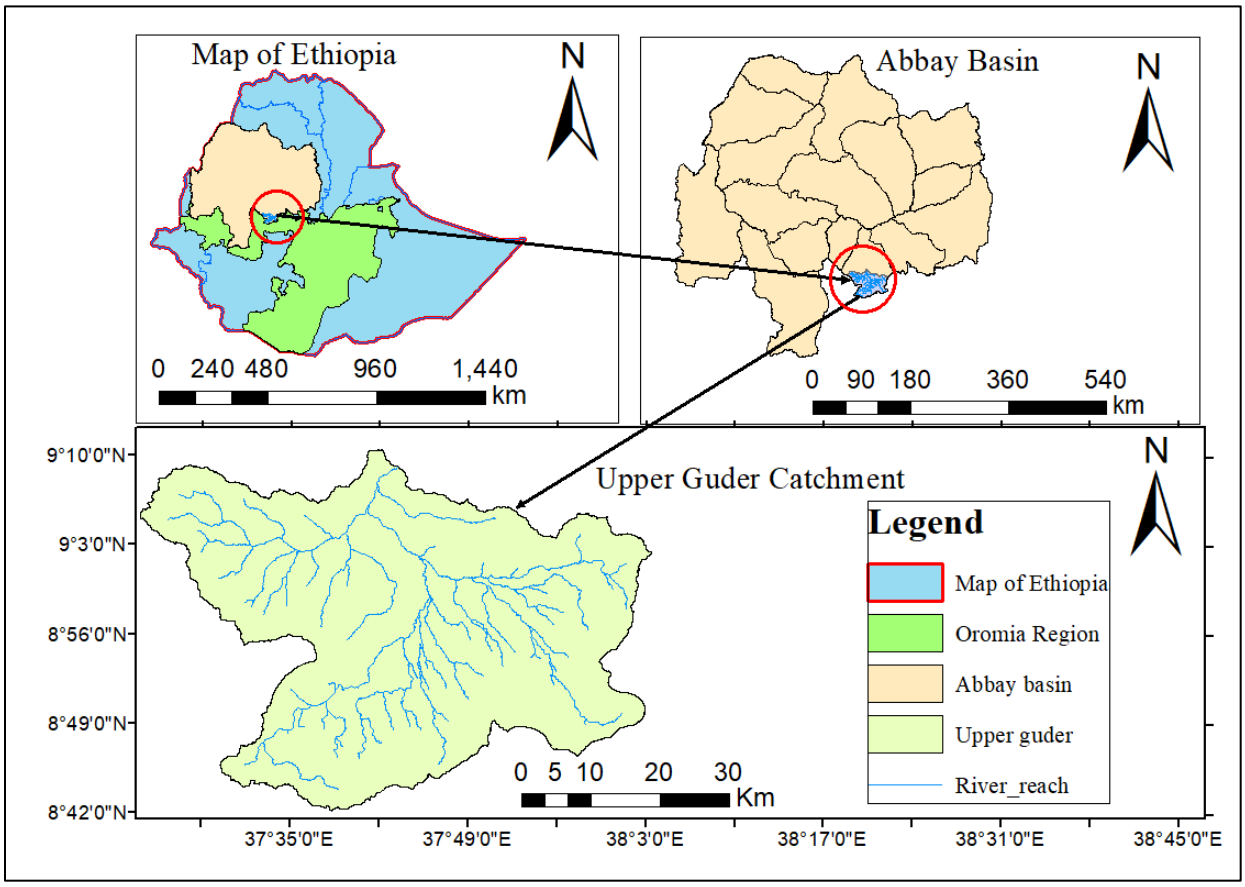

Figure 3.1: Location map of the study area

3.1.2. Topography

Upper Guder River Catchment has a drainage area of about 2290 square kilometers. The river originates from the mountainous area of the south of the towns of Ambo and Guder and the study area has mostly variable topographic range; neither steep nor flat area. The river flows from the south to the north. The digital elevation model indicated that the elevation of the Upper Guder River Catchment ranges between 1520 to 3305 meters above sea level (m. a. s. l.). The higher elevation ranges are located on the mountainous area at the South of the town of Ambo and Guder and the lower elevation are at the outlet.

3.1.3. Climate

Upper Guder River Catchment, has a comparatively mild climate because of its high elevation (1520 - 3305m. a. s. l.). The annual climate may be divided into a rainy and dry season. The rainy season may be divided into a major rainy season (Kiremt) and minor rainy seasons (Belg & Tsedey). During Kiremt season from June through August above 75% of the total rainfall occurs and in Belg season from March to May small rainfall occurs. The dry seasons (Bega) occur in December to February and Tsedey covers from September through November.

Temperature:

According to the data obtained from the national metrological agency of Ethiopia (NMASE) indicated the average annual maximum and minimum temperature in the Catchment varies between 22.58^0C – 27.69^0C and 7.12^0C – 12.16^0C respectively.

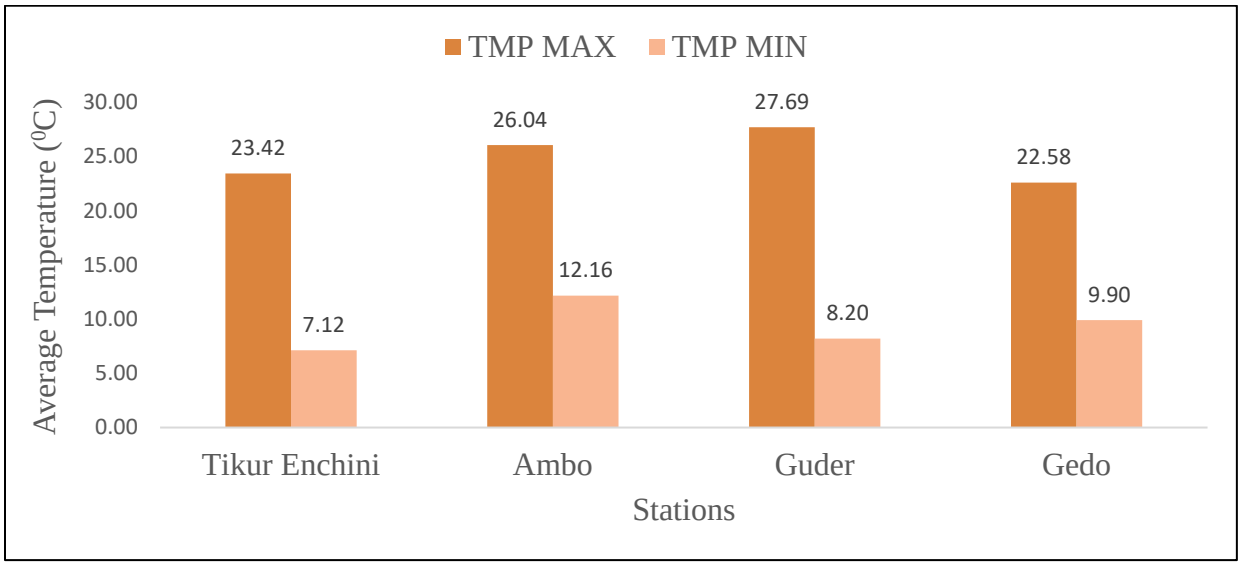

Figure 3.2: Mean annual maximum and minimum temperature in Upper Guder River Catchment (1989-2018)

Rainfall:

The catchment has an annual rainfall of ranging from 931.82mm at Gedo meteorological gauging station and 1830.85 mm at Tikur Enchini stations (from NMASE). The mean annual rainfall was stated as follows.

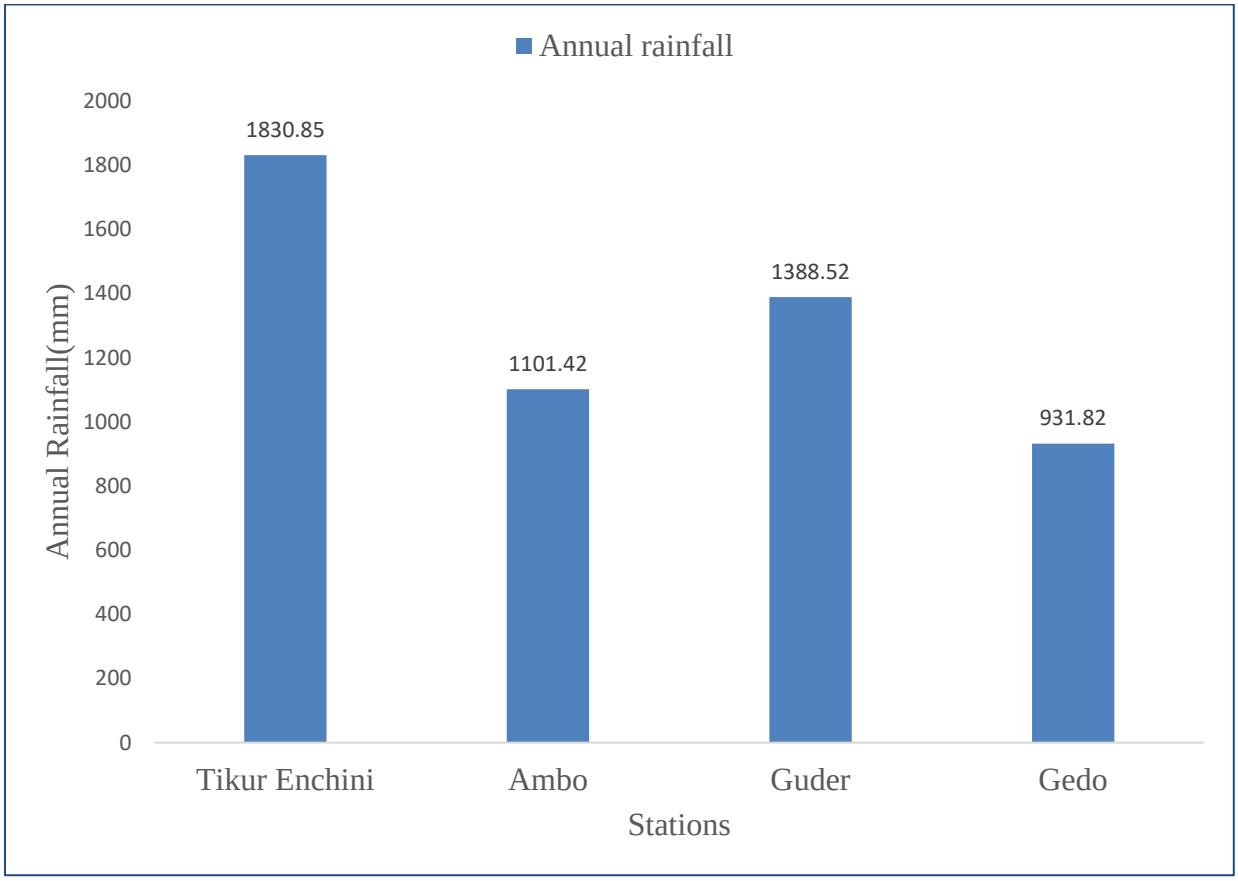

Figure 3.3: Annual rainfall of Upper Guder River Catchment (1989-2018)

3.1.4. Soil Type

Soil data was extracted from Abbay basin master plan developed by Ministry of Water, Irrigation, and Energy. The study watershed contains 10 soil types across the area at different coverage.

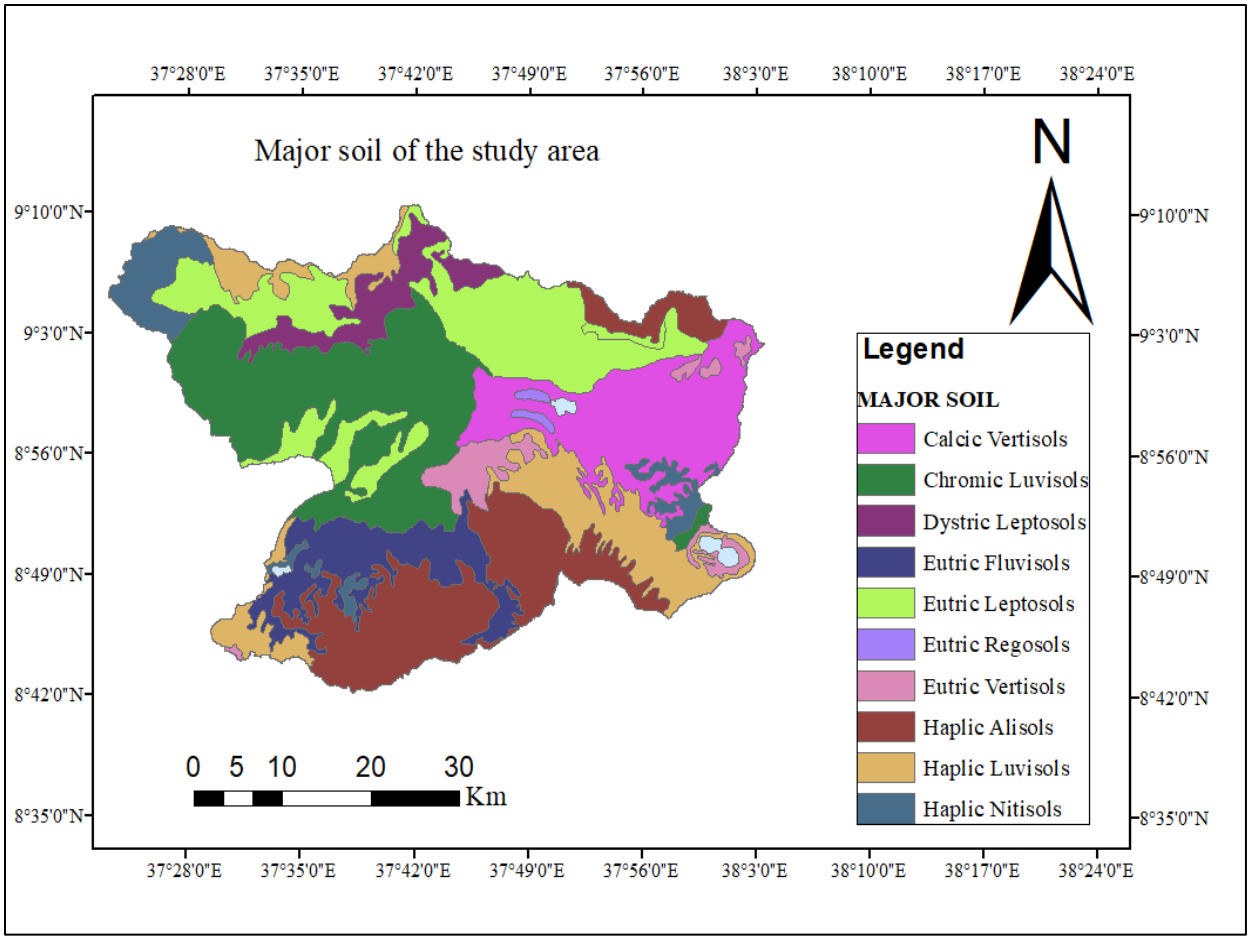

Figure 3.4: The soil map of the study area (MOWIE, 2000)

For each soil type SWAT code was assigned and used to define HRU of the model. SWAT model requires soil chemical and physical properties such as soil texture, available water content, hydraulic conductivity, bulk density, and organic carbon content for different layers of each soil type. To integrate the soil map with the SWAT model, a user soil database that contains textural and chemical properties of soil was prepared for each soil layer and added to the SWAT user soil databases. The symbol and areal coverage of catchment soils type are presented in (Table 3.1).

Table 3.1: The soil types of the study area

No	Major soil type	Symbol	Dominant texture	Area	
				Ha	%
1	Calcic Vertisols	VkVr	Clay loam	30496.78	13.32
2	Chromic Luvisols	RxLv	Clay loam	47207.24	20.61
3	Dystric Leptosols	RdLp	Clay	10372.87	4.53
4	Eutric Fluvisols	ReVr	Loam	17734.37	7.74
5	Eutric Leptosols	V/SeLp	Loam	38859.16	16.97
6	Eutric Regosols	ReRg	Loamy sand	962.47	0.42
7	Eutric Vertisols	AeVr	Clay	7684.18	3.35
8	Haplic Alisols	RhAl	Clay loam	38617.10	16.86
9	Haplic Luvisols	V/ShLv	Clay loam	26079.83	11.39
10	Haplic Nitisols	RhNT	Clay loam	11023.91	4.81
	Total			229037.92	100

3.2. Data Collection and Analyses

3.2.1. Determination of Landuse/Land Cover Change Data and Analysis

3.2.1.1. Data from Satellite Images

The image for LU/LC change has been obtained using three Landsat images; Landsat of 1989, 2002, and 2018. These Landsat images selected throughout the study period and with a cloud cover of zero were collected from U.S. Geological Survey (USGS) Center for Earth Resources Observation and Science (EROS) via node of (https://earthexplorer.usgs.gov/). The image data files were downloaded in zipped files from the Global land cover facility (GLCF) website and extracted to Tiff format files. The acquisition dates, sensor, path/row, and resolution of satellite images used in this study were summarized in the table below.

Table 3.2: The acquisition dates, sensor, path/row, and resolution of the satellite images

Satellite name	Sensor	Path/raw	Reference data	Date of acquisition	Pixel size
Landsat 05	Landsat TM	169/054	1989	Jan/04/1989	30m*30m
Landsat 05	Landsat TM	169/054	2002	Feb/25/2002	30m*30m
Landsat 08	Landsat ETM+	169/054	2018	May/12/2018	15m*15m

3.2.1.2. Image Processing and Classification

Each land sat image was georeferenced to WGS_84 datum and Universal Traverse Mercator (UTM) Zone 37N. Preprocessing images such as layer stacking and band color combination were carried out. The satellite image of each band stacking was processed using Remote Sensing (RS) software packages by ERDAS IMAGINE2014 software. Then the study area was clipped from the stacked images using ERDAS IMAGINE2014. To make a better view of surface features clearly, the satellite images were performed by color composition. Then the resampling image was required to make the same pixel size for 2018 land sat to 30m*30m, this was good for the overlay of a pixel.

Image classification was the process of assigning pixels of a continuous raster image to the predefined land cover classes. Different issues to keep in mind to avoid overlapping features and finish with effective classification parallel with the ground truth. The result of the classification was mostly affected by various factors such as classification methods, algorithms, collecting of training sites, etc. In most cases, the category of image classification technique was classified into three major categories: supervised, unsupervised, and hybrid. The hybrid classification technique (Teferi et al., 2010; Solomon et al., 2014), which involves unsupervised classification followed by a supervised classification technique. Unsupervised classifications were carried out using Iterative Self-Organizing Data Analysis (ISODATA) clustering algorithm (Boakye et al., 2008; Teferi et al., 2010) while supervised classifications were undertaken with the Maximum Likelihood Classification (MLC) algorithm (Solomon et al., 2014; Temesgen et al., 2014) by collecting training areas for the LU/LC classes.

For this study, the supervised classification type was applied. It was the most common type of classification technique in which all pixels with similar spectral values are automatically categorized into land cover classes or themes (Solomon et al., 2014; Temesgen et al., 2014). The supervised classification which relies on the prior knowledge of pattern recognition of the study area was used. It requires the manual identification of the point of interest areas as a reference or ground truth within the images, to determine the spectral signature of identified features.

For this study, the land cover map was produced based on the pixel-based supervised classification through the step such as: first, selecting the training sites which are typically representative for the

land cover classes. The training sites were collected based on the analyst's personal experience (actual coordinate of ground truth) and knowledge of the physiographical area from Google Earth, and Google Map of each year. Also, image enhancement and composition were applied for better discriminating the land cover classes. Using these approaches 210, 205, and 200 training areas were collected from each image (1989, 2002, and 2018) respectively. Second, perform the classification using the Maximum Likelihood classifier.

3.2.1.3. Landuse/Land Cover Classes

Before starting the analysis the landuse/land cover change studies usually need the development and the definition of homogeneous landuse/land cover units. These have to be differentiated using the available data source such as remote sensing, any other relevant information, and the previous local knowledge. Hence, in the study area five different types of landuse/land cover have been identified for the Upper Guder River catchment. The descriptions of these landuse/land covers are given as follows.

- ✓ Agricultural land: - areas, used for crop cultivation, both annuals and perennials. Due to the difficulty encountered in identifying the dispersed rural settlements some kind of land cover was combined with the Agricultural land during classification.
- ✓ Forest land: - land covered which includes evergreen forest land, mixed forest, and plantation forests.
- ✓ Shrub and grassland: - areas covered with shrubs, bushes, small trees, grass, pastureland, and little wood mixed with the same grass.
- ✓ Water bodies: - areas which are lake, waterlogged, and swampy throughout the year.
- ✓ Built-up Area: - area covers with Settlement areas of a building, rural residential houses, infrastructures, and roads.

The LU/LC map of the study area was coded to the SWAT four-letter codes and linked to the SWAT landuse database. This identifies the 4-letter SWAT code for the different categories of landuse/land cover would prepare to relate the grid values to SWAT landuse/land cover classes. Hence, after preparing the lookup table the landuse types were made compatible with the input required by the model.

Table 3.3: Landuse/land cover classes of Upper Guder River Catchment

No	Landuse/Land cover classes	Landuse According to SWAT Database	SWAT Code
1	Water Bodies	Water	WATR
2	Built-up Areas	Residential Medium Density	URMD
3	Shrub and Grass Land	Pasture	PAST
4	Forest Land	Forest mixed	FRST
5	Agricultural Land	Agricultural land close to grown	AGRC

3.2.1.4. Classification Accuracy Assessment and Kappa Coefficient

One of the most important final steps in the classification process was accuracy assessment. Accuracy assessment aimed to quantitatively assess how effectively the pixels were sampled into the correct land cover classes. Moreover, the key emphasis for accuracy assessment pixel selection was on areas that could be identified on both Landsat image, Google Earth, and Google Map of each year.

Depending on the goal of the accuracy assessment, the number of ground truth sample plots can be calculated with different methods, those are Binomial distribution and Rule of thumb. If the project objective was to test not only right versus wrong but also to look at the multiple classes of wrong then a Binomial distribution should be used to calculate the sample size (Rosenfield, 1982). These computations allow the calculation of overall accuracy. This function describes the probability of getting misclassifications in a sample drawn from a parametric accuracy proportion (Ginevan, 1979). However, in Rule of thumb, the number of samples for each category might be adjusted based on the relative importance of that category for a particular application. However, these techniques are not designed to choose a sample size for filling in an error matrix (Congalton, 1991). So for this study, Binomial distribution was used.

The following equation to calculate the sample number (cumulative binomial probability distribution):

$$N = \frac{Z^2 PQ}{E^2} \quad \text{.....3.1}$$

Where:

N: number of samples

Z: 2 * DS (DS: the standard deviation which was taken from metadata of classified image)

P: The expected percent accuracy,

Q = 100 − p and

E: the allowable error

In classifying 1989, 2002, and 2018 images, reference data from Google Earth and actual field (for 2018 images) corresponding periods were collected. So 184, 188, and 191 ground truth points (locations) were randomly collected for the classified image of 1989, 2002, and 2018 respectively and the result presented in the result and discussion section. Accuracy assessment was employed concerning the corresponding each year of Google Earth images to illustrate the representativeness of the classified images on the ground.

The overall accuracy gives the overall results. It was calculated by dividing the total number of correct pixels (diagonals) by the total number of pixels in the confusion matrix. The recommended standard of accuracy in the identification of LU/LC mapping from the remote sensor data should be 85%–95% (Anderson et al, 1976). The false-color composite of 1989, 2002, and 2018 images was stated in Appendix B-4, 5, and 6.

The kappa ($K^{'}$) coefficient gives the agreement between the classified image and reference or ground truth. Kappa analysis is a discrete multivariate technique used in accuracy assessments. According to (Monserud, 2003) the acceptable ranges of the kappa coefficient was presented below.

Table 3.4: Kappa statics ranges (Monserud, 2003)

Kappa statics ranges		
1	< 0.00	Poor
2	0.00 - 0.20	Slight
3	0.21 - 0.40	Fair
4	0.41 - 0.60	Moderate
5	0.61 - 0.80	Substantial
6	0.81 - 1.00	Almost perfect

The Kappa statistic was computed as;

$$K = \frac{\sum_{i=1}^{r} Xii - \sum_{i=1}^{r}(Xi+Xi+1)}{N^2 - \sum_{i=1}^{r}(Xii+Xi+1)} \quad \text{.....3.2}$$

Where;

r: number of rows and columns in the error matrix,

N: total number of observations (pixels),

Xii: observation in row i and column i,

Xi: a marginal total of row i, and

Xi+i: a marginal total of column i,

3.2.2. SWAT Model Setup and Performance Evaluation

For model setup the ARCSWAT of SWAT2012 with ArcGIS10.3 was used. SWAT model requires specific information about the catchment such as DEM, weather data, hydrological data, soil data, and landuse/land cover. These data were collected from different sources and databases. The SWAT model was set up using the data prepared and the SWAT interface. The interface helps to create the stream network, delineate the catchment boundary from the Digital Elevation Model (DEM) and further subdivide the catchment into sub-catchment. The data were collected and analyzed as presented in the next sub-sections.

3.2.2.1. Meteorological Data

Climate data was the main demanding input data for the SWAT simulation. The weather input data required for SWAT simulation includes daily data of precipitation, maximum and minimum temperature, relative humidity, wind speed, and solar radiation. These were obtained from the National Metrological Agency of Ethiopia. The weather data used were represented from four stations in the catchment. Such as Tikur Enchini, Ambo, Guder, and Gedo as shown in Table 3.5.

Table 3.5: Location of meteorological stations in the Upper Guder River Catchment (NMAE)

No	Station name	location			Metrological data					
		Lat (^{0})	Long (^{0})	Elevation	Rainfall	TMP max	TMP min	HMD	WND	SLR
1	Ambo	8.99	37.84	2068	√	√	√	√	√	√
2	Gedo	9.02	37.46	2520	√	√	√			
3	Guder	8.96	37.86	2011	√	√	√			
4	Tikur Enchine	8.84	37.67	2467	√	√	√			

Ambo station was the first class that has records of all climatic variables. The first contains variables like maximum and minimum temperature, humidity, sunshine hours, and wind speed in addition to rainfall. Whereas the rest three (Tikur Enchini, Guder, and Gedo) was the second class stations (Table 3.5). The second group contains only rainfall, Maximum and Minimum temperature data.

The climatic data used for this study was covers 30 years from 1989-2018. However, missing values were identified in some of the climatic variables. These values were assigned with no data code (-99) which when filled by the weather generator embodied in the SWAT model from monthly weather generator parameter values. The monthly generator parameters values were estimated from the weather stations (Ambo station). Finally, the weather data were prepared in txt format with lookup tables as required by the model.

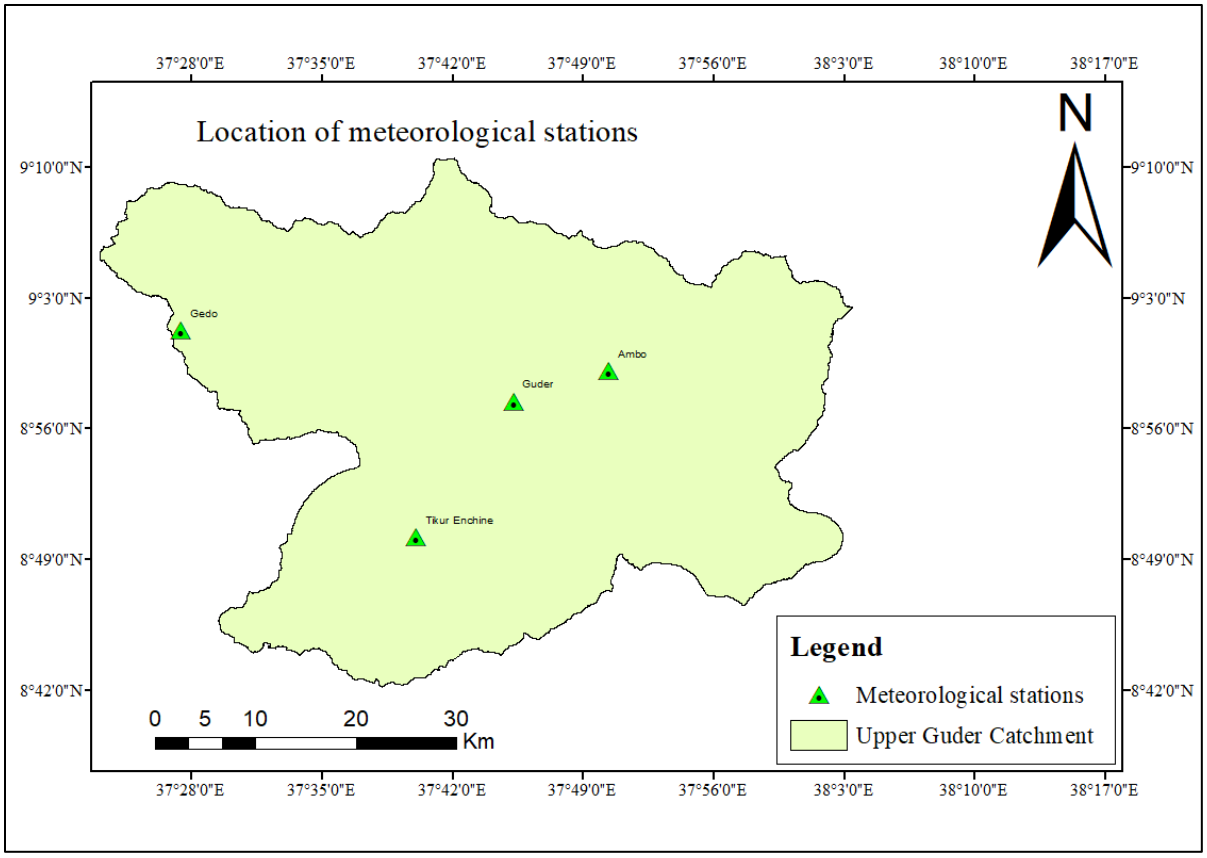

Figure 3.5: Location of meteorological stations used in the Upper Guder River Catchment

3.2.2.2. Hydrological Data

The flow data was also collected from the Ministry of Water, Irrigation, and Energy of Ethiopia (MOWIE). As the following Table 3.6 indicates there were three gauging stations were found at upstream of Guder River. As per the Ministry of Water, Irrigation and Energy of Ethiopia (MOWIE) data indicates from those Fatto and Indris gauging station has no long recorded data. So those stations were used only for filling missing data for Guder gauging station; the missing data were filled by using the regression method for Guder gauging station.

Table 3.6: Location of the streamflow gauging stations

No	Station Name	latitude	longitude
1	Guder Nr. Guder	8.95	37.75
2	Fatto Nr. Guder	8.87	37.74
3	Indris Nr, Guder	8.937	37.743

Regression provides a means of finding the values of the coefficients a and b for straight line;

$y = a + bx$……..……3.3

The coefficients a and b can be found by the least square method using two simultaneous equations;

$$\left.\begin{aligned}\sum y &= na + b\sum x \\ \sum xy &= a\sum x + b\sum x^2\end{aligned}\right\}$$……..…..3.4

Where; y = monthly rainfall, x= annual rainfall, n = number of year

The flow data at Guder gauging station were arranged as per the requirement of the SWAT_CUP software. Flow data was required for sake of calibration and validation of the model. The flow data at Guder has only a period of 15 years from 1995 to 2009.

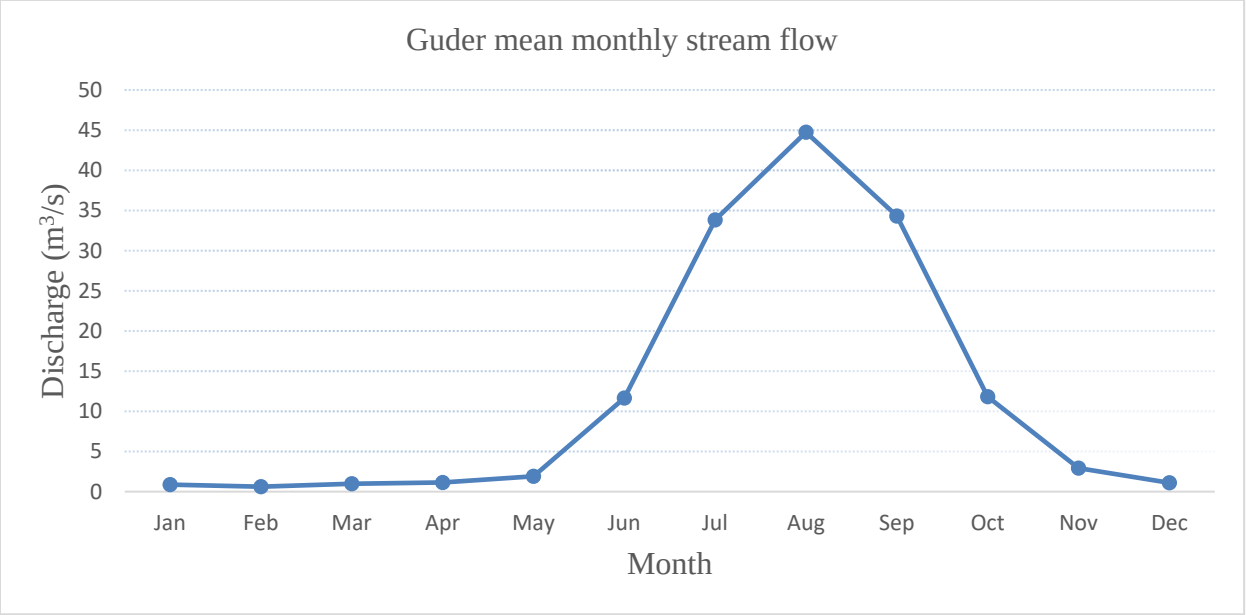

Figure 3.6: Mean monthly discharge of Guder River (1995-2009)

3.2.2.3. Filling Missing Data

Missed measured precipitation data may face many problems in hydrologic analysis and design. Because of the cost associated with data collection and some natural and man-made conditions sometimes make it very difficult to have complete records of data at every station. Conditions above mentioned sometimes prevent to obtain quantitative and qualitative data of the study area. For gauges that require periodic observation, the failure or absence of the observer to make the necessary visit to the gauge, destruction of recording gauges, and instrument failure because of mechanical or electrical malfunctioning can result in missing data. Any such causes of instrument failure reduce the length and information content of the precipitation record. Hence, there are

different methods for filling the missing data, from those methods station-average method and the normal ratio method was used for the rainfall in this study area (Richards, 1998).

When the average catches were differed by more than 10%, the normal ratio method (equation 3.5) was preferable. That means if at least one station was outside the range the normal ratio method was used.

$$Px = \frac{1}{n} * \left(\left(\frac{Nx}{N1}\right) * P1 + \left(\frac{Nx}{N2}\right) * P_2 + \cdots + \left(\frac{Nx}{Nn}\right) * P_n\right) \quad \text{3.5}$$

Where;

Px: the missing data at station x

Nx: the missing data stations normal annual rainfall

Ni: normal annual rainfall at station i. and

n: number of nearby gauges.

The station-average method for estimating missing data uses n gauges from a region to estimate the missing point rainfall, Px, at another gauge:

$$Px = \frac{1}{n} \sum_{i=1}^{n} Pi \quad \text{3.6}$$

Where; Pi: the rainfall at gauge i

(Equation 3.6) was accurate when the total annual rainfall at any of the n regional gauges when the mean of percent difference with in the 10%. This method gives equal weight to the rainfall at each of the regional gauges. The value 1/n was the weight given to the rainfall at each gauge used to estimate the missing rainfall. Therefore before using the data it was first essential to apply a gap-filling technique.

3.2.2.4. Homogeneity Test

Homogeneity analysis was used to separate a change in the statistical properties of the time-series data. The causes can be either natural or man-made. These include alterations to landuse and relocation of the observation gauging station. Therefore, to select the representative meteorological station checking homogeneity of group stations was essential, the homogeneity of the selected gauging stations daily rainfall records was carried out by non-dimensional equation (Tadesse, 2016):

$$Pi = \frac{Pim}{Pm} \quad \text{3.7}$$

Where:

Pi: Non-dimensional Value of precipitation for the month i

Pim: Over the years averaged monthly precipitation for the station i

P_m: Over year's average yearly precipitation of the station P

According to Homogeneity test analysis, the selected stations were plotted for comparison with each other; Figure below shows the result of the homogeneity analysis result. The same-mode and pattern of the stations are observed and hence group stations selected are homogenous.

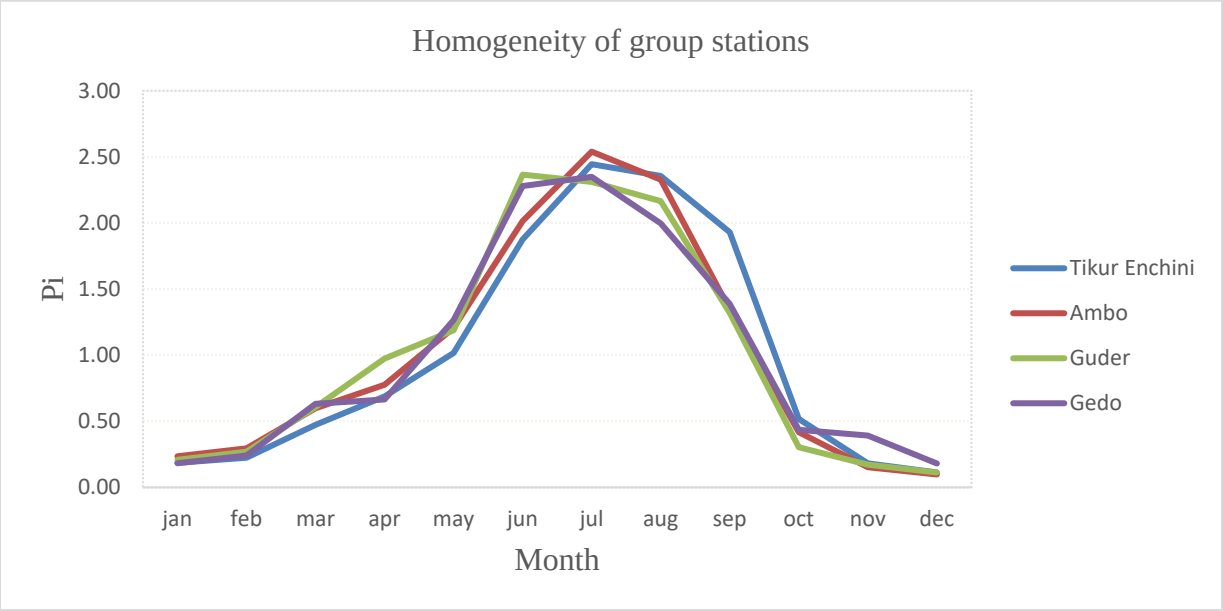

Figure 3.7: Homogeneity test analysis for all rainfall stations

3.2.2.5. Consistency of Rainfall Data

A Double Mass Curve (DMC) was used to check the consistency of rainfall for adjustment of inconsistent data. This technique was based on the principle that when each record data comes from the same parent sample, they are consistent. A group of four base stations in the neighborhood of the station was selected. A consistent record is one where the characteristics of the record have not changed with time. A double-mass curve is a graph of the cumulative catch of rain gauge of interest versus the cumulative catch of one or more gauge in the region that has been subjected to a similar hydro metrological occurrence and was known to be consistent. If the rainfall record was a consistent estimator of the hydro-meteorological occurrences throughout the record, the double-mass curve will have a constant slope. A change in the slope of the double mass curves would suggest that an external factor has caused changes in the character of the measured values. If the

change in slope was evident, then either the record needs to be adjusted with the early or the later period of record adjusted if greater than 10% (Hardision, 1960).

$$\frac{Pa}{Pd} = \frac{\frac{Y}{X}}{\frac{Yd}{Xd}} = \frac{Slope\ of\ original\ line}{Slope\ of\ deviated\ line} = Correction\ factor \quad \text{.....3.8}$$

In which:

Pa = adjusted amount

Pd = deviated amount for the concurrent period for which pa is desired.

According to the double mass curves analysis, all the stations in the Upper Guder River Catchment were consistent. The double mass curves for all stations are presented below.

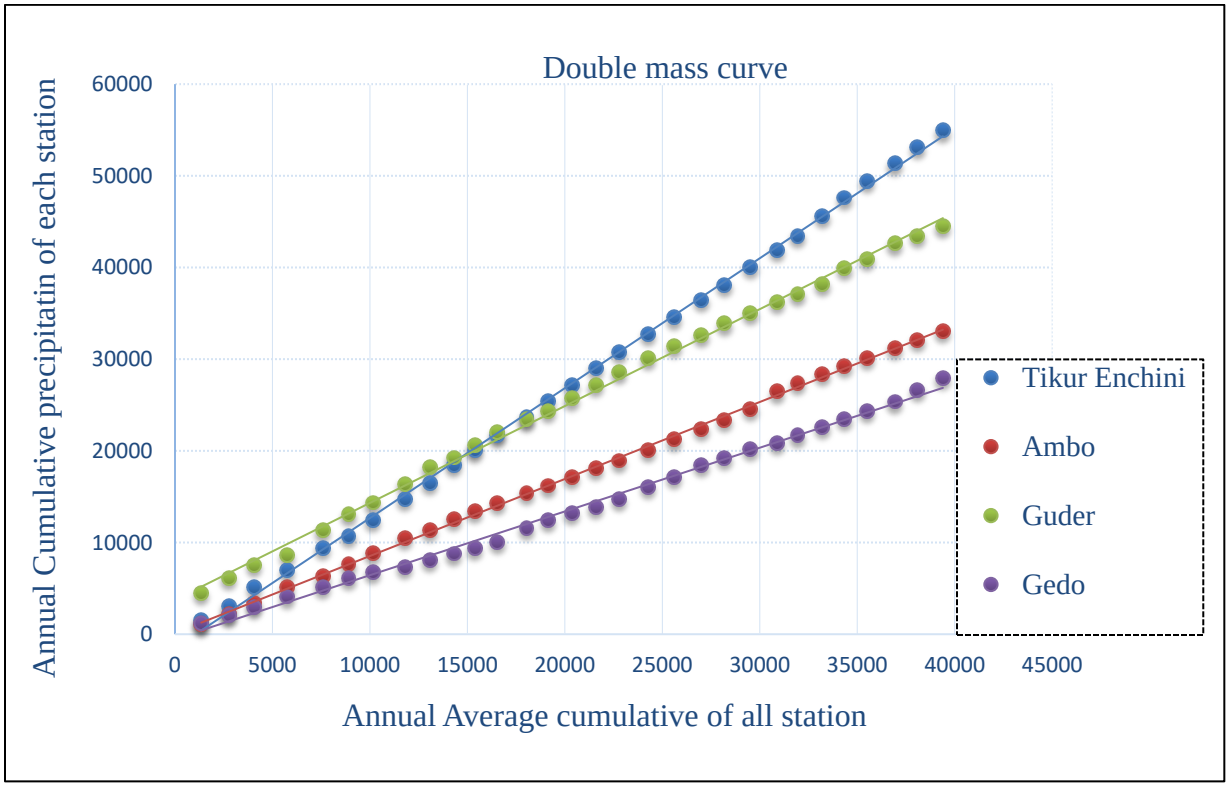

Figure 3.8: Double mass curve of all rainfall stations

3.2.2.6. Weather Generator

To generate the data, SWAT Weather Database was designed to be a friendly tool to store and process daily weather data to be used with SWAT projects. It was capable of storing relevant daily weather information, easily by creating .txt files to be used as input information. During a SWAT project setup efficiently calculating the WGEN statistics of several weather stations in one-step run (Essenfelder, 2016). As for any SWAT project, missing values must be entered as -99. Such

values will not be used during the calculation of the WGEN statistics. They will, however, be written to the SWAT input .txt files (Essenfelder, 2016).

The weather generator parameters were developed by using excel (pivot table), to calculate average monthly and average daily precipitation, standard deviation, skew coefficient, probability of a wet day following a dry day, and an average number of days of precipitation in a month. After HRU analysis the weather data to be used in a watershed simulation was imported using the first command in the Write Input table's menu item on the SWAT toolbar. This tool helps to load weather station locations into the current project and assign weather data to the sub-watersheds. The weather data definition was divided into six tabs: weather generator data, rainfall data, temperature data, solar radiation data, wind speed data, and relative humidity data. In developing countries, there was a lack of a full and realistic long period of climatic data. Therefore, the weather generator solves this problem by generating data from the observed one (Danuso, 2002).

The Model requires the daily values of all climatic variables from measured data or generated from values using monthly average data over several years. This study used measured data for all climatic variables. Weather data of one station (Ambo) with continuous records were used as input to determine the values of weather generator parameters. Hence, for weather generator data definition, the weather generators data file WGEN_user, rainfall data, temperature data, relative humidity data; solar radiation data, and wind speed data were selected and added to the model respectively. Lastly next to the added input tables run the simulations daily.

3.2.2.7. Watershed Delineation

Digital Elevation Model (DEM) data was required for watershed delineation, to calculate the flow accumulation and stream networks using SWAT watershed delineator tools. A 30m by 30m resolution ASTER Global Digital Elevation Model was obtained from the MOWIE.

The watershed delineation processes consist of five major steps, DEM setup, stream definition, outlet and inlet definition, watershed outlet(s) selection definition, and calculation of sub-basin parameters. Once, the DEM setup was completed and the location of the outlet was specified on the DEM, the model automatically calculates the flow direction and flow accumulation. Subsequently, stream networks, sub-watersheds, and topographic parameters were calculated using the respective tools.

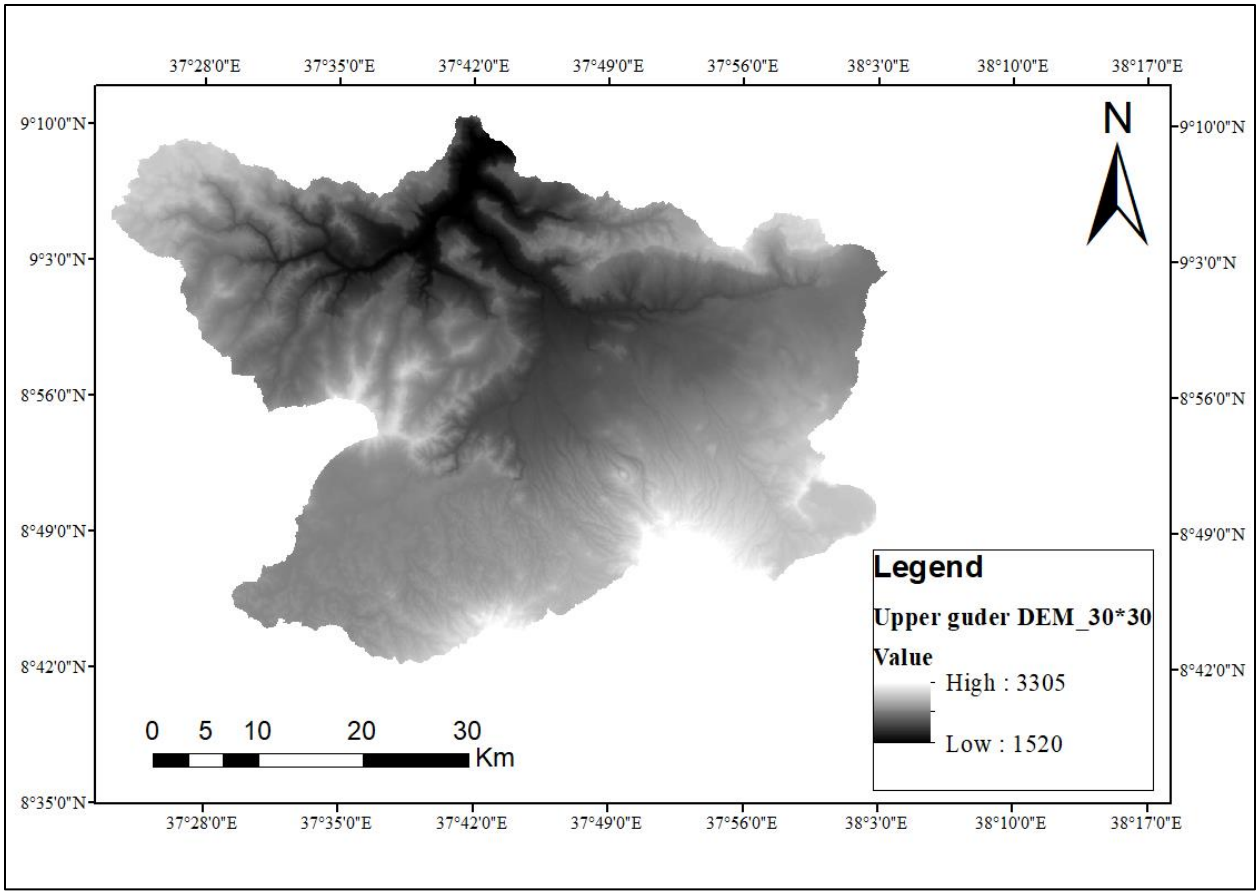

Figure 3.9: DEM of Upper Guder River Catchment (MOWIE)

The stream definition and the size of sub-basins were carefully determined by selecting the threshold area or minimum drainage area required to form the origin of streams. Using threshold value by the SWAT interface (7000ha), the Upper Guder River Catchment was delineated into 21 sub-basins having an estimated total area of 2290km^2 (Figure 3:11).

During the watershed delineation process, the topographic parameters (elevation, slope) of the watershed and its sub-watershed were also generated from the DEM data. Accordingly, the elevation of the watershed ranges from 1520 to 3305 above mean sea level, the high elevation was at the Mountain and the lowest at the Catchment outlet.

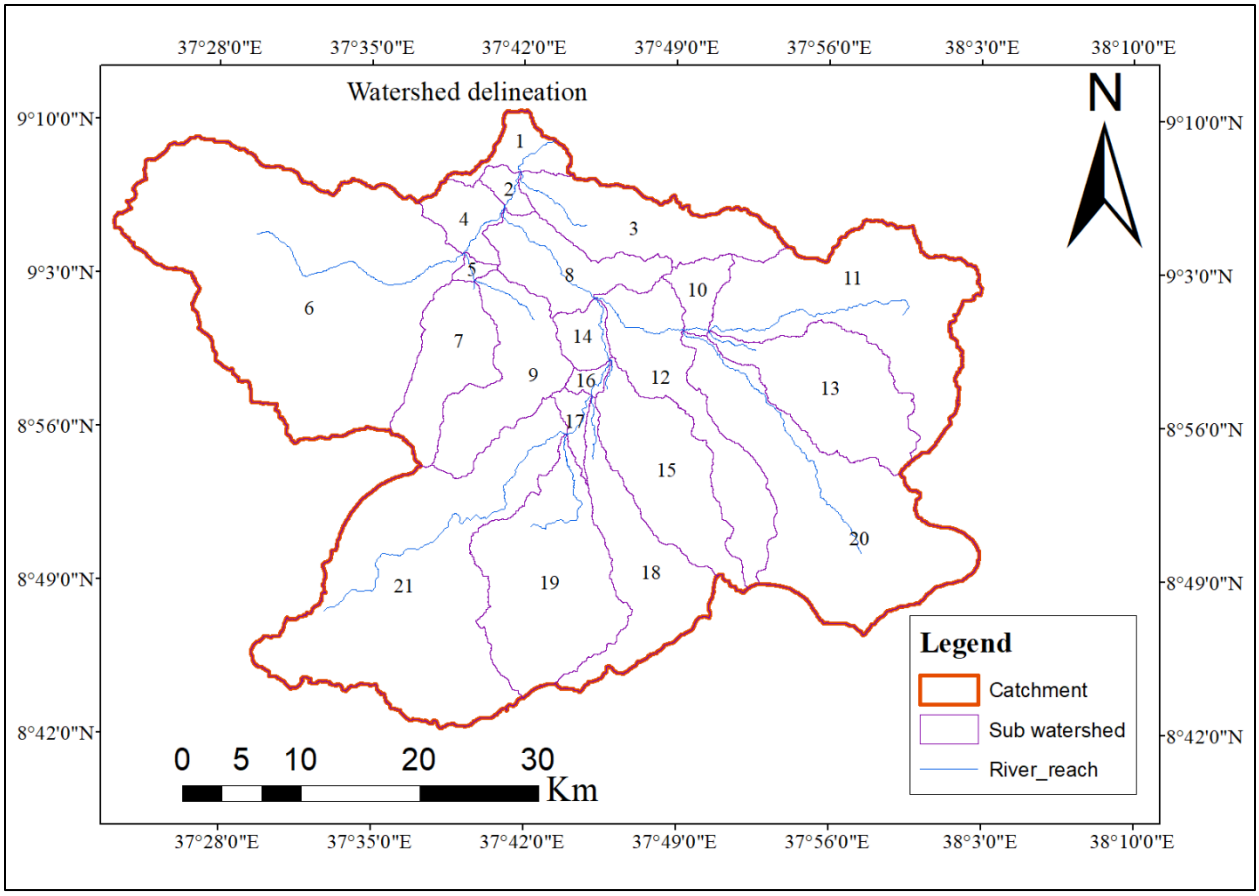

Figure 3.10: Watershed delineation of the study area using SWAT

3.2.2.8. Hydrologic Response Units

The sub-watershed was divided into HRUs by assigning the threshold values of landuse/land cover, soil, and slope percentage. These tools allowed loading landuse and soil maps which are in raster formats into the current project, evaluates slope characteristics, and determining the landuse/soil/slope class combinations in the delineation of the sub-basin. Slope classification was carried out based on the height range of DEM used during watershed delineation. The slope values of the watershed were classified in percent. It was reclassified into four classes (0 -2, 2-5, 5-8 and >8) as recommended by the FAO slope definition (FAO, 1999).

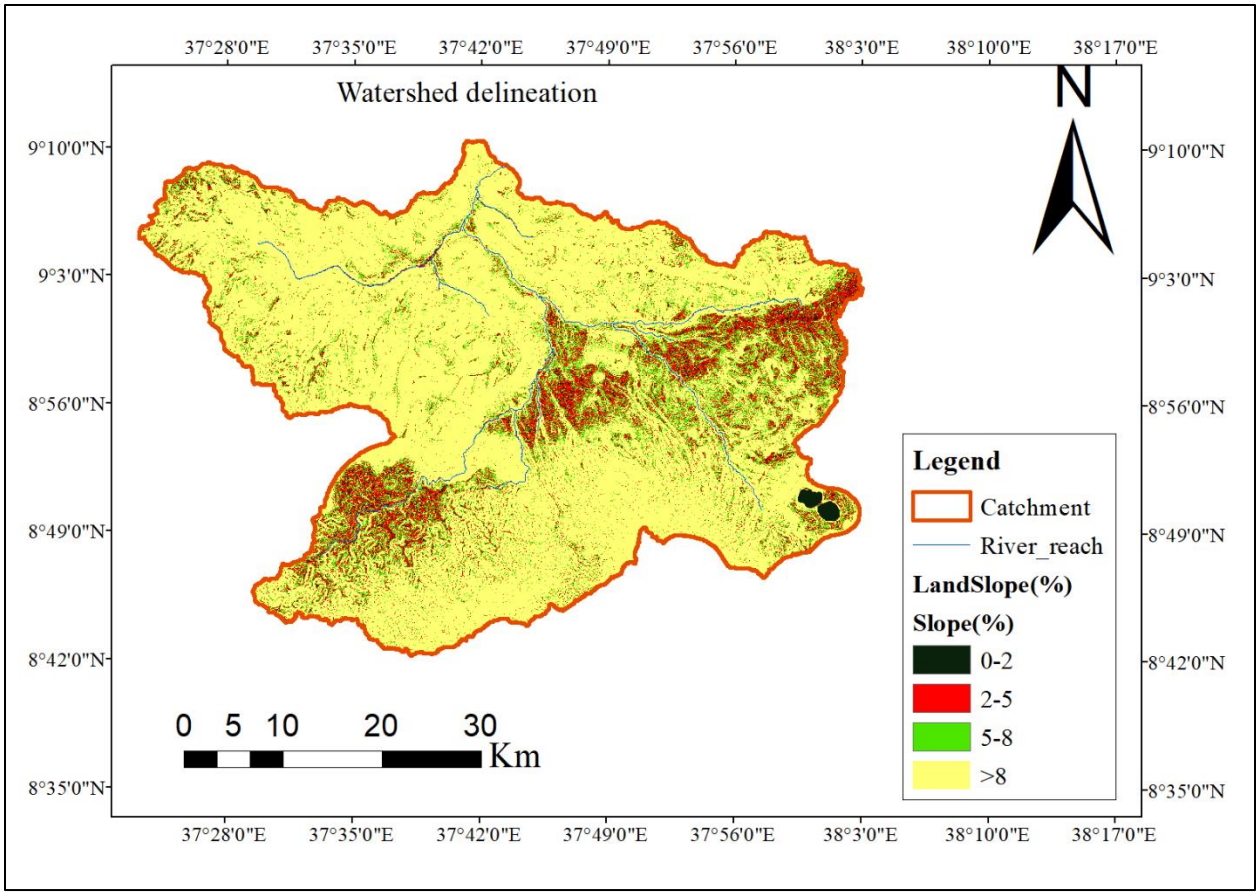

Figure 3.11: Slope class of study area

In general, the threshold level is used to eliminate minor landuse/land covers in sub-basin, minor soil within landuse/land cover area, and minor slope classes within a soil on specific landuse/land cover area. Following minor elimination, the area of remaining landuse/land covers, soils, and slope cases are reapportioned so that 100% of their respective area modeled by SWAT. Landuse, soil, and slope characterization for the Sub-basin were performed using commands from the HRU analysis menu on the SWAT Toolbar.

In the model, there are two options in defining HRU distribution, assign a single HRU to each sub-basin, or assign multiple HRUs to each sub-basin based on certain threshold values. For this study, HRU definition with multiple options accounts based on the model setup with land use, soil and slope, and minimum area threshold values set as 5% landuse, 10% soil, and 10% slope threshold combination was used. These threshold values indicate that landuse which form at least 5% of the sub-basin area and soils which form at least 10% of the area within each of the selected landuse will be considered in HRU. Hence, the sub-basins were divided into 245, 205, and 173 HRUs for

1989, 2002 and 2018 landuse/land covers respectively; each has a unique landuse and soil combinations. The number of HRUs varies within the sub-watersheds.

3.2.2.9. Sensitivity Analysis

Before the calibration and validation process, a sensitivity analysis was carried out to reduce the number of parameters that need optimization (Arnold et al., 2012). In this research semi-automated Sequential Uncertainty Fitting (SUFI 2) was used to identify the sensitive parameters. This was done to select the most flow influencing parameters in the catchment. Two kinds of sensitivity analyses are performed, local (one at a time) and global analysis. The sensitivity of one parameter often depends on the value of other related parameters, which was a problem with local sensitivity analysis. Global analysis requires a large number of simulations which can also be a problem. In this research global sensitivity analysis was performed in SUFI-2 before calibration and the results were examined. However, in this research, the number of simulations used for calibration was 500, which was large enough to get accurate results for global sensitivity analysis. The global sensitivity analysis approach was used in SUFI-2 because it takes into account the sensitivity of one parameter relative to the other to give their statistical significance (Arnold et al., 2012).

In the sensitivity process, the SWAT simulated TxtInout was copied to the working directory and SWAT_CUP SUFI-2 was used for performing the sensitivity of selected parameters with the default lower and upper parameter bounds. The 12 parameters were included for the sensitivity analysis with default values as recommended by SWAT_CUP SUFI-2. Upon completion of sensitivity analysis, t-stat was used to identify the relative significance of each parameter. The larger the absolute value of t-Stat and the smaller the p-Value, the more sensitive the parameter. That means a predictor that has a low p-value was likely to be a meaningful addition to the model because changes in the predictor's values are related to changes in the response variable. Conversely, a large p-value suggests that changes in the predictor are not associated with changes with the response. So that the parameter was not very sensitive. A p-value of less than 0.05 was generally accepted point at which to reject the null hypothesis (Van Griensven, 2006). Based on the above criteria, parameters were selected for the calibration process and the results were presented in the result and discussion section.

The streamflow data of fifteen years from 1995-2009 of the catchment gauging station were used to compute the sensitivity of streamflow parameters. In the sensitivity process, by entering the

SWAT interface SWAT-CUP sensitivity analysis window, first, the SWAT simulation was specified for performing the sensitivity analysis and the location of the sub-basin where observed data was compared against simulated output. Then, selected parameters were entered for sensitivity analysis with the default lower and upper parameter bounds. And the rank of sensitivity was based on the value of t-stat and p-values (Van Griensven, 2006).

In this study, the t-Stat and P-Values of the parameters were used to rank the different parameters that may influence the flow and finally to select the ranked values. For this analysis, 12 parameters were selected based on previous literature (Kidane et al., 2018) and only 6 parameters were identified to have a significant influence in controlling the streamflow in the watershed. Flow parameters that are tested for their sensitivity values are stated in (Table 4.9).

3.2.2.10. Model Calibration and Validation

Following the sensitivity analysis result, model calibration was done to obtain optimum values for sensitive parameters. SWAT provides three options for calibration: manual calibration, auto-calibration, and combination of these two methods. For this study, first manual calibration was done to fine-tune some of the parameters, and some model parameters were adjusted by manual calibration. Model calibration was computed using the 2002 LU/LC map, because this map was found within the range of observed streamflow data (1995-2009). Then, auto-calibration by SWAT-CUP was done on daily time steps using the measured streamflow data of the catchment. It was recommended that to allocate more measured data (about 2/3) for calibration (Abbaspour et al., 2015), so the measured daily streamflow data of ten years from 1995-2004 were used for the model calibration process.

There were different calibration procedure methods Generalized Likelihood Uncertainty Estimation (GLUE), Parameter Solution (ParaSol), Sequential Uncertainty Fitting (SUFI2), and Markov chain Monte Carlo (MCMC). For this study, the Sequential Uncertainty Fitting (SUFI2) option was selected. This method was chosen for its applicability to both simple and complex hydrological models. SUFI-2 was superior over other algorithms because it involves stochastic calibration, where the errors and uncertainties in the model are recognized and expressed as ranges accounting for all driving variables. The inclusion of a large number of parameters representing different processes in the objective function, in SUFI-2 helps to make the model result enveloping most of the observations well. For example, (Asres and Awulachew, 2010) were used SWAT in

Gumera Watershed, Ethiopia for runoff and sediment modeling, and in calibration, they were used two approaches. Fully automated Parameter Solution (ParaSol) and semi-automated Sequential Uncertainty Fitting 2 (SUFI-2). They were carried out calibration using thirteen runoff producing parameters and concluded that the best performance of SUFI-2 and its flexibility over ParaSol and gave higher values for the coefficient of determination (R^2) and NSE coefficient.

In this procedure, by entering the SWAT interface SWAT_CUP Auto-calibration window, first, the SWAT simulation was specified for performing the auto-calibration and the location of the catchment where observed data could be compared against simulated output. After the auto-calibration runs completed, the model was run using the best parameter output values and the simulations were compared with observed streamflow data using Nash and Sutcliffe coefficient of efficiency (NSE) and coefficient of determination (R^2).

Validation was also done to compare the model outputs with an independent data set without making further adjustments to the parameter values. Model validation is the comparison of model outputs with an independent data set without making further adjustments which may adjust during the calibration process. The measured daily streamflow data of five years from 2005-2009 were used for the model validation process. In this process, the two model performance values were also checked here to make sure that the simulated values are still within the accurate limits.

To compare the 95PPU band with a discharge signal, we devised two statistics referred to as p-factor and r-factor (Abbaspour et al., 2015). P-factor was the percentage of measured data bracketed by the 95% prediction uncertainty (95PPU) and another measure quantifying the strength of a calibration/uncertainty analysis was the R-factor, which was the average thickness of the 95PPU band divided by the standard deviation of the measured data and is a measure of the quality of the calibration. Its value should ideally be near zero, indicating small uncertainty bound of prediction (Abbaspour et al., 2015). These measurements are within the simulation uncertainty of our model; hence, they are simulated well and accounted for by the model. The results of the streamflow gauged stations of the P-factor and R-factor was shown in Table 4.10.

3.2.2.11. Model Performance Evaluation

For evaluation of model performance during calibration and validation statistical measures as well as graphical representation were used (Arnold et al., 2012). For this study, the statistical parameters

(R^2, NSE, and PBIAS) were used for model evaluation for quantification of accuracy in Catchment modeling. Each method was ranked by model performance values (NSE, PBIAS, and R^2) at each time interval (daily, monthly, and annual) (Arnold et al., 2012). For this study, the daily time interval was used, because the daily values of all climatic variables data were used for SWAT input over several years.

Table 3.7: Model performance ratings to evaluate the SWAT model (Moriasi et al., 2013).

Performance Rating	NSE	PBIAS (%)	R^2
Very good	$x > 0.75$	$\|x\| < 10$	$x > 0.80$
Good	$0.65 < x \leq 0.75$	$10 \leq \|x\| < 15$	$0.70 < x \leq 0.80$
Satisfactory	$0.50 < x \leq 0.65$	$15 \leq \|x\| < 25$	$0.60 < x \leq 0.70$
Unsatisfactory	$x \leq 0.50$	$\|x\| \geq 25$	$x \leq 0.60$

3.2.3. Effects of Landuse/Land Cover Change on Stream Flow

The main goal of this study was to evaluate the impact of landuse/land cover change on the streamflow in the case of Upper Guder River Catchment. LU/LC of the catchment was an important distinctive physical impact in the catchment surface runoff process that affects erosion rate, soil infiltration capacity, and evapotranspiration. Understanding the impacts of historic LU/LC systems have had on river flow was required to understand the future effects they have on hydrological regimes at a different level of a catchment. LU/LC of 1989, 2002, and 2018 was used to run the model by keeping other model parameters the same. The three landuse/land cover maps, soil, climatic, and streamflow data values were used to evaluate the impact of landuse/land cover change on streamflow using the SWAT model.

To perform a comparison to study change the models were calibrated using the six most sensitive parameters and validated using the same best-fitting parameter values. To evaluate the impact the model simulated three times using constant parameter values in all simulations. Once the streamflow was simulated using the SWAT model, the impact was computed by comparing each flow together. The impact of LU/LC change was quantified as the difference between simulation one and three. After calibration and validation for Guder stream flow, three independent simulations were run to evaluate streamflow variability due to landuse/land cover change. The 1989, 2002, and 2018 landuse/land cover were used as input variables in the SWAT model to

compare output as a result of their differences in landuse/land cover change. The seasonal streamflow variability of 1989, 2002, and 2018 due to landuse/land cover change was assessed and comparison was made on streamflow based on the simulation outputs.

The bellow figure indicates the general workflow followed to model the impact of LU/LC on streamflow of the upper Guder River Catchment.

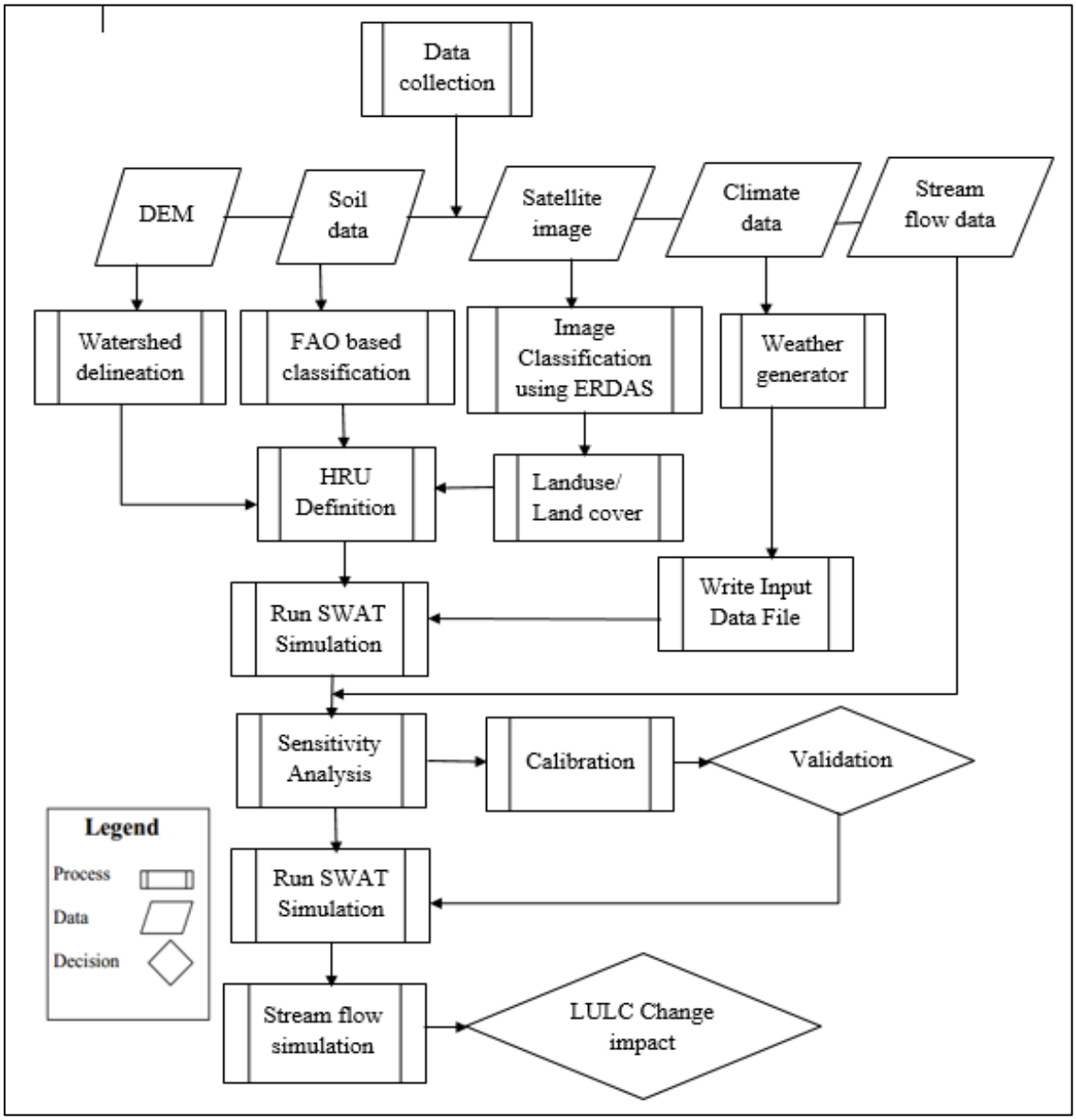

Figure 3.12: General framework followed in this study

4. RESULTS AND DISCUSSION

4.1. Landuse/Land Cover Change Detection

LU/LC change trend in Upper Guder River Catchment was analyzed from multi-temporal Landsat images for the last three decades (1989 -2018) and the associated impact of this change on streamflow was quantified using the SWAT model. Five major landuse classes were identified such as water body, forest land, shrub and grassland, agricultural land, and built-up area. In all classification periods, agricultural land accounted for more than 61.51% of the total catchment area, which was more than half of the total land area. Whereas, forest land and shrub and grassland decreased with 6.48% and 4.23% respectively with the study period (Table 4.8). This value shows clearly that agriculture plays an important role in the socio-economic development of the study catchment. Figure 4.1, 4.2, 4.3 respectively and Table 4.7 shows the LU/LC classification and distribution in the catchment over thirty (30) years in three times series (1989, 2002, and 2018).

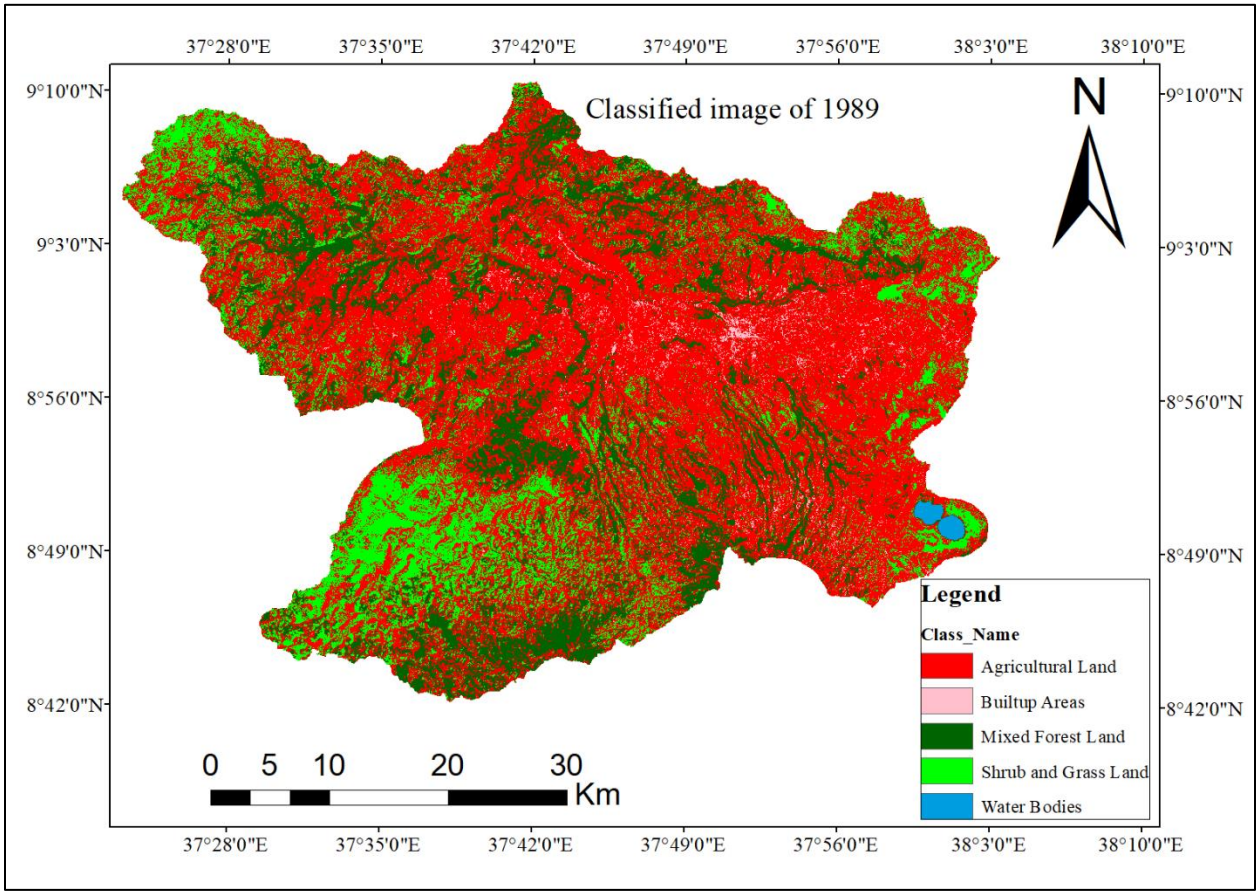

Figure 4.1: The classified image of 1989

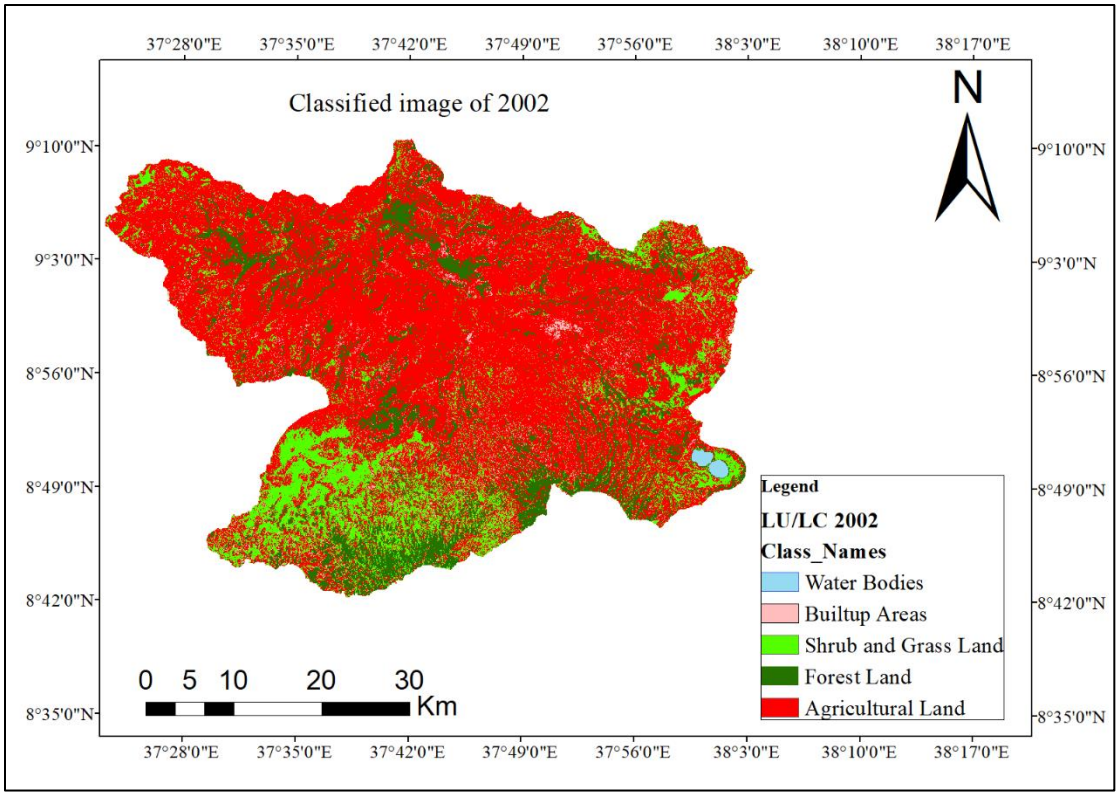

Figure 4.2: The classified image of 2002

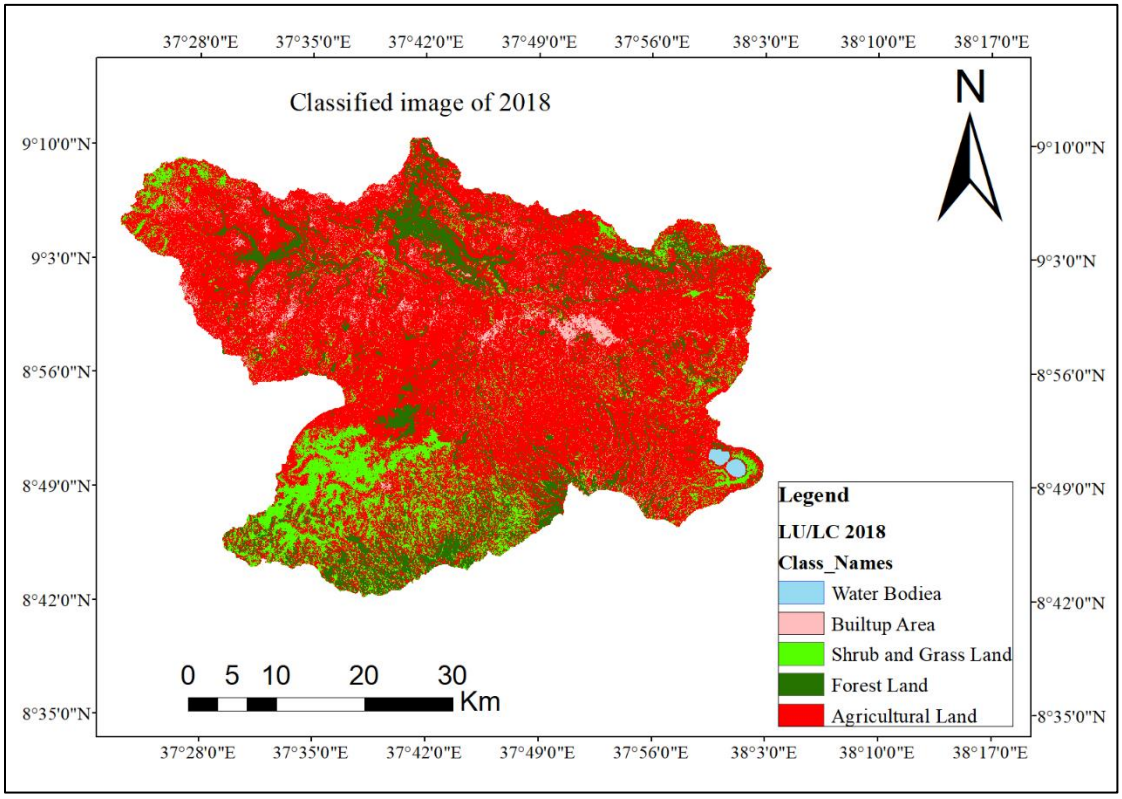

Figure 4.3: The classified image of 2018

4.1.1. Accuracy Assessment

Using the original stacked image and the Google Earth Image of each year as a reference, randomly selected points were compared with the corresponding classification. So 184, 188, and 191 points were selected for the validation of 1989, 2002, and 2018 images respectively. Table 4.1, 4.3, and 4.5 shows accuracy assessment for the three Landsat images.

Overall accuracy:

The results show that the overall accuracy for the maps of 1989, 2002, and 2018 was 88.59%, 90.43%, and 92.15% respectively. According to (Anderson et al., 1976), the minimum accuracy value for reliable land cover classification was 85%. Therefore, based on Table 4.1, 4.3, and 4.5 the classification carried out in this study produces an overall accuracy that fulfills the minimum accuracy level defined by Anderson for those land cover maps of Upper Guder River Catchment.

Producer's Accuracy:

Indicate how well training set pixels of the given cover type are classified and tells us how well a certain area can be classified. It was obtained by dividing the number of correctly classified pixels in the category by the total number of pixels of the category in the reference data. It gives only the proportion of correctly classified pixels. The overall result of the producer's accuracy ranges from 66.67% to 95.35%. The lowest values were misclassified due to the similar spectral value of different land cover classes. For instance, Waterbody with forest, Agricultural land with forest cover, Agricultural land during the dry season with Built-up area (which is classified as Built-up area), etc. somehow affects the level of classification.

User's Accuracy:

Indicate the probability that a pixel classified into a given category represents that category on the ground. It was the ratio between the total number of pixels correctly belonging to a class (diagonal elements) and the total number of pixels assigned to the same class by the classification procedure. This quantity describes the probability that a pixel of the classified image truly corresponds to the class to which it has been assigned. In this study, the user's accuracy ranges from 68.18% to 100%. The lowest value "Built-up Areas" was, to some extent, misclassified because of the similarity spectral properties of Built-up Areas and Agricultural Land.

Kappa coefficient:

A Kappa coefficient equal to 1 means perfect agreement whereas a value close to zero means that the agreement was no better than would be expected by chance. The results indicated that the Kappa coefficient for the maps of 1989, 2002, and 2018 from Table 4.2, 4.4, and 4.6 were 0.836, 0.857, and 0.886 respectively for each year. Therefore, according to Table 3.4, the classification carried out in this study produces the Kappa statics ranges between 0.81-1.0 with the almost perfect agreement for the year of 1989, 2002, and 2018.

Table 4.1: Confusion matrix for the classification of 1989

Classified Data	Reference Data						
	WB	BUA	SHGL	FRST	AGRC	Row Total	Users Accuracy
WB	2	0	0	0	0	2	100.00%
BUA	0	15	1	2	4	22	68.18%
SHGL	0	0	30	0	4	34	88.24%
FRST	1	0	3	43	1	48	89.58%
AGRC	0	2	0	3	73	78	93.59%
Column Total	3	17	34	48	82	184	
Producers Accuracy	66.67%	88.24%	88.24%	89.58%	89.02%		
Overall Classification Accuracy = 88.59%							

Overall Kappa Statistics = 0.8364

Note: AGRC=Agricultural land; WB = Water Body; FRST = Forest land, SHGL = Shrub and Grassland; BUA = Built Up.

Table 4.2: Condition of Kappa (k^) statistics for each category

Class Name	Kappa
Water Bodies	1
Built-up Areas	0.6494
Shrub and Grassland	0.8557
Forest Land	0.8591
Agricultural Land	0.8844

Table 4.3: Confusion matrix for the classification of 2002

Classified Data	Reference Data						
	WB	BUA	SHGL	FRST	AGRC	Row Total	Users Accuracy
WB	2	0	0	0	0	2	100.00%
BUA	0	19	0	0	2	21	90.48%
SHGL	0	0	23	1	5	29	79.31%
FRST	1	0	0	43	0	44	97.73%
AGRC	0	3	3	3	83	92	90.22%
Column Total	3	22	26	47	90	188	
Producers Accuracy	66.67%	86.36%	88.46%	91.49%	92.22%		
Overall Classification Accuracy = 90.43%; Overall Kappa Statistics = 0.8577							

Table 4.4: Condition of Kappa (k^) statistics for each category

Class Name	Kappa
Water Bodies	1
Built-up Areas	0.8921
Shrub and Grass Land	0.7599
Forest Land	0.9697
Agricultural Land	0.8123

Table 4.5: Confusion matrix for the classification of 2018

Classified Data	Reference Data						
	WB	BUA	SHGL	FRST	AGRC	Row Total	Users Accuracy
WB	2	0	0	0	0	2	100.00%
BUA	0	26	0	0	1	27	96.30%
SHGL	0	0	31	0	2	33	93.94%
FRST	1	0	0	35	1	37	94.59%
AGRC	0	2	2	6	82	92	89.13%
Column Total	3	28	33	41	86	191	
Producers Accuracy	66.67%	92.86%	93.94%	85.37%	95.35%		
Overall Classification Accuracy = 92.15%; Overall Kappa Statistics = 0.8863							

Table 4.6: Condition of Kappa (k^) Statistics for each category

Class Name	Kappa
Water Bodies	1
Built-up Area	0.9566
Shrub and Grass Land	0.9267
Forest Land	0.9312
Agricultural Land	0.8023

4.1.2. The magnitude of Landuse/Land Cover Change

The three classified landuse/land cover maps of 1989, 2002, and 2018 were generated from the Landsat TM and ETM+ imaginary classification (Figure 4:1, 4:2, and 4:3 respectively). In the catchment, the area covered by different landuse/land cover in percent was described in Table 4.7.

The catchment result showed that the massive change was recorded between Agricultural land, shrub and grassland, and forest land. It was easily shown that there was an increase of Agricultural land, built-up area and water bodies, and decrease of forested areas, and shrub and grassland over 30 years in selected three times series (1989, 2002, and 2018). So Agricultural land, shrub and grassland and forest dominated the catchment during the study period, and the Built-Up area and water body were also the parts of the catchment. For detailed information presented in Table 4.7.

In general, during the three landuse/land cover maps period, the Agricultural land increased at about 8.04%, and Built-up area increased by 2.69%, whereas the Shrub and grassland decreased by 4.23% and also forested area decreased by 6.48% (Table 4.8). For the individual class area and change statistics of the three periods are summarized in Table 4.7.

Table 4.7: Magnitude and proportion of LU/LC

Class name	1989		2002		2018	
	Area(km^2)	% of proportional	Area(km^2)	% of proportional	Area(km^2)	% of proportional
Water Bodies	6.70	0.29	7.01	0.31	7.08	0.31
Built-up Areas	34.79	1.52	67.66	2.95	96.31	4.21
Shrub and Grass Land	387.00	16.90	334.85	14.62	290.06	12.66
Forest Land	452.79	19.77	348.17	15.20	304.42	13.29
Agricultural Land	1408.79	61.51	1532.76	66.92	1592.87	69.55
Total	2290	100	2290	100	2290	100

Several other studies in and around Blue Nile Basin particularly in the Upper Blue Nile (Abdo et al., 2009 and Amare & Kameswara, 2012) suggested aspects of the farming systems, institutional settings, environmental policy, and several other factors have been modifying the catchment LU/LC in the basin. It was shown that there was an increased in Agricultural land and a decreased in forested areas, shrub and grassland. Thus the current study was in agreement with other studies conducted in Ethiopia (Tolessa et al., 2016; Welde and Gebremariam, 2017 and Gashaw et al., 2018).

Table 4.8: LU/LC change by percentage area from 1989-2018

Class name	LU/LC by percentage			LU/LC change Area in percentage		
	1989	2002	2018	2002-1989	2018-2002	2018-1989
Water Bodies	0.29	0.306	0.309	0.02	0.003	0.02
Built-up Areas	1.52	2.95	4.21	1.44	1.25	2.69
Shrub and Grass Land	16.90	14.62	12.66	-2.28	-1.95	-4.23
Forest Land	19.77	15.20	13.29	-4.57	-1.91	-6.48
Agricultural Land	61.51	66.92	69.55	5.41	2.63	8.04

4.2. Evaluation of the SWAT Model Performance

4.2.1. Sensitivity Analysis of Flow Parameters

For global sensitivity analysis, twelve (12) flow parameters that may affect streamflow were selected and only 6 parameters were identified to have a significant influence in controlling the streamflow in the catchment. Table 4.9 indicated the relative sensitive parameters for the flow of stream affecting the hydrologic process of Upper Guder River Catchment and used in model calibration

A total of 12 parameters with 500 number of simulations were done at Guder gauged station to select the rank of these parameters. Van Griensven et al., (2006), characterized Global rank 1 as "very important", rank 2 to 6 as 'important", rank 7 to 19 as "slightly important" and rank 27 as "not important". Appendix A-3 shows the relative sensitivity rank of parameters concerning the Guder gauged stations. The parameters were allowed to vary during the calibration process within acceptable ranges across the catchment until an acceptable fit between the measured and simulated values was obtained at the catchment gauge outlet; no changes were made to the calibrated parameters during the 5-year validation simulation.

Table 4.9: SWAT model fitted parameter values for daily calibration

No	Parameter Name	Description	Fitted Value	Absolute value range
1	CN2	SCS runoff curve number f	55.85	35 - 98
2	GW_DELAY	Groundwater delay (days)	17.50	0 - 500
3	ESCO	Soil evaporation compensation factor	0.89	0 -1
4	SLSUBBSN	Average slope length	122.67	10 - 150
5	OV_N	Manning's "n" value for overland flow	29.37	0 - 30
6	CH_N2	Manning's "n" value for the main channel	0.03	0.02 - 0.30
7	SOL_AWC	Available water capacity of the soil layer	0.37	0 - 1
8	ALPHA_BNK	Base flow alpha factor for bank storage	0.05	0 - 1
9	SFTMP	Snowmelt base temperature	7.48	-20 - 20
10	SURLAG	Surface runoff lag time	14.64	0.05 -24
11	SOL_BD	Moist bulk density	1.84	0.9 -2.5
12	GW_REVAP	Groundwater "revap" coefficient.	0.17	0.02 - 0.2

The result of the sensitivity analysis indicated that the most sensitive parameters were Manning's "n" value for overland flow (OV_N.hru) with a t-value of 43.02 and p-value of 0 to simulate Guder catchment and the least sensitive was Surface runoff lag time (SURLAG.bsn) with absolute t-value of 0.21 and p-value of 0.83.

4.2.2. Calibration and Validation

Calibration was computed using 1995 – 2004 daily climate data with 2 years warm-up period against measured discharge data. Model validation consists of the comparison of the model outputs with an independent data set without making further adjustments to the parameters obtained during the calibration process. Generally, model calibration entails the modification of parameter values and comparison of the output of interest to measured data until model efficiency was achieved (James and Burges, 1982).

The calibration and validation were demonstrated by the coefficient of determination (R^2), Nash-Sutcliffe simulation efficiency (NSE), and percent of bias (PBIAS). The measured and simulated streamflow for the catchment were obtained Statistical agreement between simulated and observed flow data during the calibration periods resulted in a very good and good agreement using R^2 and NSE with the result of 0.84 and 0.74 respectively. Both values for the Guder gauged stations fulfilled the acceptable requirement of $R^2 > 0.6$ and NSE > 0.5, which was recommended by (Santhi, 2001). Based on the result, the model was efficient enough to represent and evaluate the impact of LU/LC change on streamflow variability (Table 4.10).

Using the same parameter values of the calibrated model setup were validated and found to prove the applicability and result of acceptable performance. Model validation was performed from 2005 to 2009 against the daily measured due date value. The validation in terms of streamflow results was evaluated for respective years (2005–2009) in terms of R^2 and NSE were 0.83 and 0.72 respectively; which shows a very good and good agreement between the simulated and observed data respectively. The percent of bias (PBIAS) describes the tendency of the simulated data to be greater or smaller than the observed data, expressed as a percentage. Negative values were indicative of the best estimation. The result indicates as recommended by (Santhi, 2001), it reveals the very good performance of the model.

Table 4.10: Daily calibration and validation of model performance with uncertainty analysis

Criteria		Calibration	Validation
Coefficient of determination (R^2)		0.84	0.83
Nash–Sutcliffe efficiency (NSE)		0.74	0.72
Percent of bias (PBIS)		-6.9	-9.5
uncertainty analysis	P-factor	0.64	0.43
	R-factor	0.08	0.08

P-factor was the percentage of measured data bracketed by the 95% prediction uncertainty (95PPU) and another measure quantifying the strength of a calibration/uncertainty analysis was the R-factor, which should ideally be near zero, indicating small uncertainty bound of prediction (Abbaspour et al., 2015).

As seen from the calibration and the validation results, the model represented the hydrological characteristics of the catchment at Guder gauging stations and can be used as a baseline for further analysis.

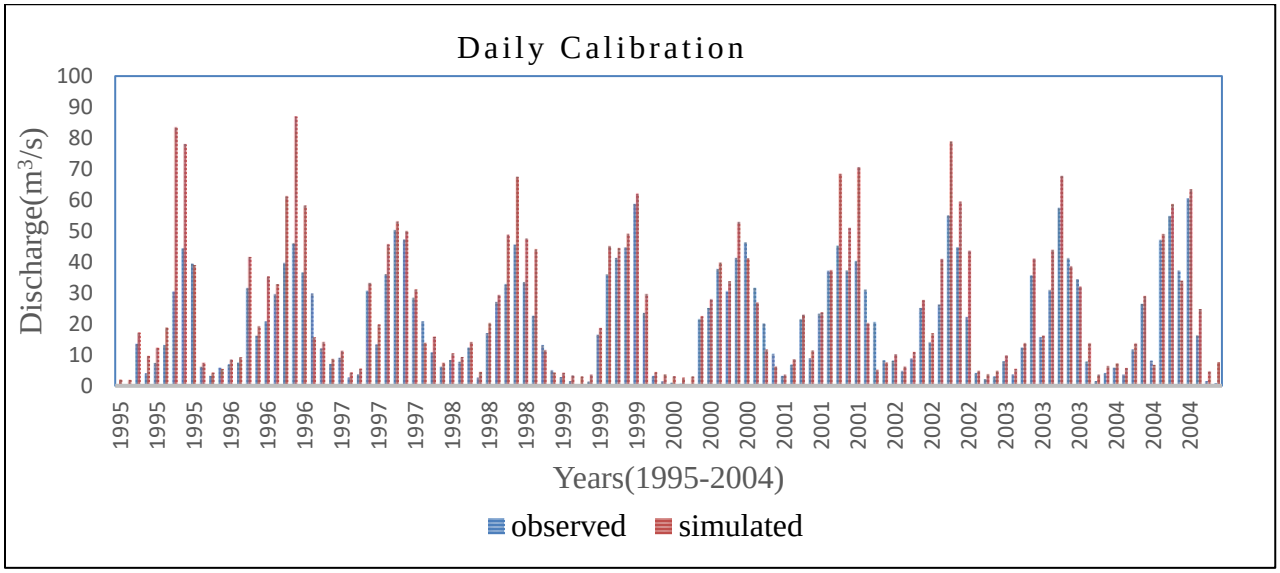

Figure 4.4: Simulated and observed discharge for daily calibration period (1995-2004)

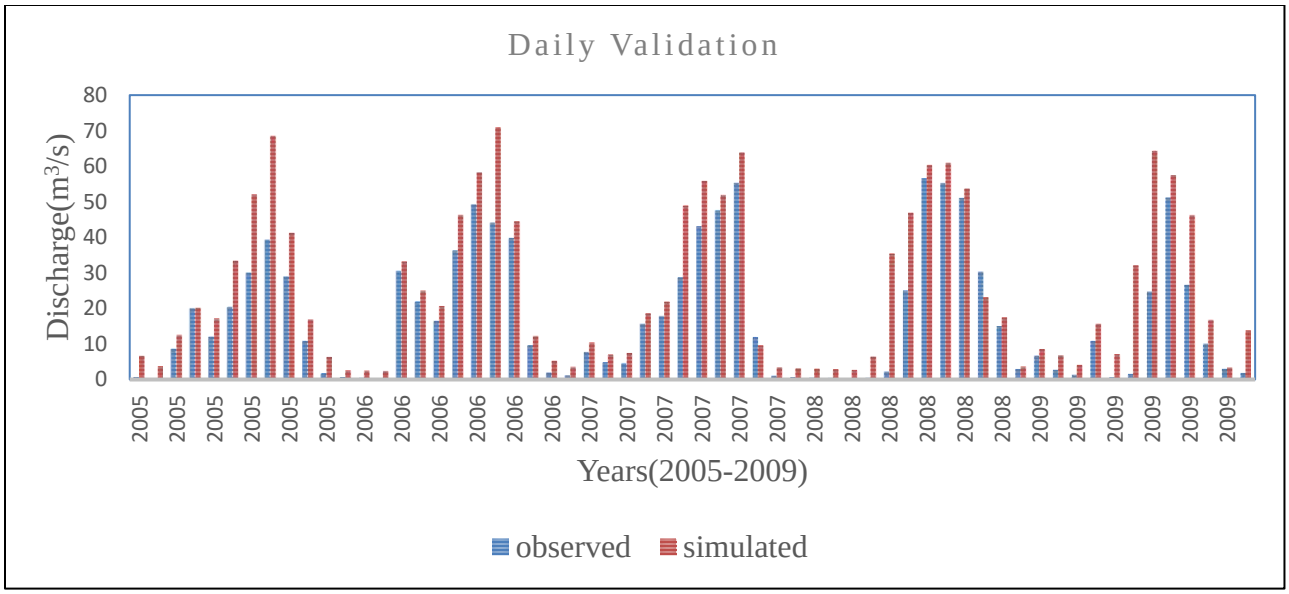

Figure 4.5: Simulated and observed discharge for daily validation period (2005-2009)

Generally, the graphical and statistical results both during the calibration and validation period showed adequate model performance, but the model over predicted may be due to local rainfall storms that were not well represented by the rainfall data used in the hydrologic simulation because of uneven weather stations distribution and some missing data, and also the quality of observed data may affect.

4.3. The effects of Landuse/Land Cover Change on Stream Flows

The Outflow of the outlet catchment was computed and compared with each other and it shows a significant variation. The result of 1989, 2002, and 2018 LU/LC change, immediate effect on streamflow was summarized in four flow periods; dry season, wet season, short rainy season, annual and total together with annual and total flow daily recorders (Table 4.11). The simulated streamflow for the 2018 LU/LC result revealed that the flow was increased by 5.25% and 10.04% during short rainy and wet season respectively. This result can be characterized as a positive impact (increasing streamflow) to the flow record because of LU/LC change in the catchment. Whereas; the result also simultaneously shows a negative (decrease in streamflow) impact on the dry season which contributes to a decrease in the streamflow by 6.60%. The percentage of change was done when 2018 LU/LC compared with 1989 LU/LC.

Table 4.11: Mean monthly simulated streamflow change due to LU/LC change

Flow season	Simulated streamflow			2002-1989	2018-2002	2018-1989	% of change
	1989	2002	2018				
Dry season (m^3/s)	34.49	33.53	32.21	-0.96	-1.32	-2.28	-6.60
short rainy season (m^3/s)	47.07	48.16	49.54	1.09	1.38	2.47	5.25
wet season (m^3/s)	149.59	152.48	164.61	2.89	12.14	15.02	10.04
Annual flow (m^3/s)	77.05	77.06	87.32	0.01	10.27	10.27	13.33

Note: Dry season extend from December to February; short rainy season extends from March to May; wet season extends from June through August; Yearly/annual streamflow that extends from January to December.

LU/LC change has significant impacts on streamflow in all the study periods. This result was supported by past studies in the Upper Blue Nile Basin at the different temporal and spatial contexts (Kidane et al., 2018; Gashaw et al., 2018). This can be explained by a massive increment of agricultural land for different farming activities to support the rapid population growth at a cost of forest and shrub. The changes in LU/LC had a significant impact on determining the amount of streamflow (Mwangi et al., 2016).

For assessing change in the contribution of streamflow components due to LU/LC change, the analysis was made. As it can be seen from the bellow Table 4.12, the simulated SURQ and GW_Q using the 2018 LU/LC result revealed that the surface runoff was increased by 5.73% and the groundwater contribution was decreased by 2.26% when it was compared with 1989 LU/LC (the negative result shows the decreased of GWQ). The variation was associated with the landuse/land cover change during the study period. This was attributed to the expansion of agricultural land and urbanization over forest land and pasture land that results in the increase of surface runoff following rainfall events and causes variation in soil moisture content and groundwater storage. The percentage of change was done when 2018 LU/LC compared with 1989 LU/LC.

Table 4.12: Mean annual simulated surface runoff and groundwater flow

Flow season	LU/LC change			Difference			
	1989	2002	2018	2002 -1989	2018-2002	2018-1989	% change
SURQ(mm)	21.04	21.81	22.24	0.77	0.43	1.21	5.73
Lateral Q(mm)	16.25	16.17	15.94	-0.08	-0.23	-0.31	-1.91
percolation to shallow aquifer (mm)	53.14	52.71	52.05	-0.43	-0.66	-1.09	-2.05
GW_Q (mm)	2.66	2.63	2.60	-0.03	-0.03	-0.06	-2.26

As stated by Turner et al., (1993) and Tracy et al., (2007), from past studies Surface runoff recorded in the area of cultivation and grassland, was much higher than forest area. Cultivation land can keep less soil moisture and higher runoff than forests. Therefore the rainfall quickly satisfies the soil moisture in cultivation land and converted to rapidly runoff in areas where cultivation land was dominant. Forest land can intercept the rainfall by a canopy structure and gives the water more time to satisfy soil moisture and infiltrate to the ground which decreases the amount of waters to generate runoff (Scott et al., 2002; Teferi et al., 2010). Decreasing forest vegetation cover, expansion of cultivation land, and urbanization at a cost of natural forest are known causes to increase streamflow during the wet and short rainy season. While it decreases the base flow during the dry season by decreasing infiltration, which reduces the amount of water to be percolated to recharge the groundwater.

5. SUMMARY AND CONCLUSION

5.1. Summary

The study integrated GIS with SWAT hydrological model to model the impact of LU/LC changes on the streamflow of Upper Guder River Catchment. GIS and remote sensing data analysis help in studying the catchment LU/LC change for the last 30 years (1989–2018). The LU/LC classification of the catchment identifies five classes for 1989, 2002, and 2018 satellite images.

The analysis of the three images shows that the study catchment has recorded a significant spatial and temporal LU/LC change throughout the last 30 years. The massive change was recorded between Agricultural land, shrub and grassland, and forest land. During classification of 1989 were Agricultural land, forest land, shrub and grassland, converted from 61.51%, 19.77% and 16.90 % to 66.92%, 15.20% and14.62 % during 2002 respectively and lastly, during 2018 it was converted to 69.55% Agricultural land, 13.29% forest land and 12.66% shrub and grassland. The result of this analysis showed that the Agricultural land has expanded during the study period of 1989-2018. During the study period, forest land and shrub and grassland decreased by 6.48% and 4.23% while, Agricultural land and Built-up area increased by 8.04% and 2.69% respectively.

For hydrological modeling, the sensitivity analysis was done and the most sensitive parameter of 6 was selected using SWAT CUP automated sensitivity analysis. The calibration and validation result evaluated using statistical models of R^2, NSE, and percent of bias (PBIAS) model efficiency, and the SWAT model show the required performance. The Model Performance for both calibration and validation of the study catchment was found to be acceptable with the coefficient of determination (R^2) values of 0.84 and 0.83 and Nash–Sutcliffe coefficients (NSE) values of 0.74 and 0.72 respectively.

After effective model calibration and validation, the impact of landuse/land cover change on streamflow was assessed. The result of the model for 1989, 2002, and 2018 were computed and compared by classifying streamflow period into four (dry season, wet season, short rainy season, and annual). The study showed a positive impact (increasing streamflow) resulted from LU/LC change in the catchment; which increased by 5.25% and 10.04% during short rainy and wet season respectively. Whereas; the result also depicted that change in LU/LC has a negative impact (decrease in streamflow) on the dry season which contributes to a decrease in the streamflow by

6.60% when compared with 1989 LU/LC. Additionally, the SURQ increased by 5.73% while GWQ decreased by 2.26% due to the increment of Agricultural land. The model results showed that the streamflow characteristics changed due to the land cover changes during the study period. In General, the study catchment was experiencing a significant LU/LC change which in turn affects the streamflow. This kind of result should pay particular attention to land use policy and management in the catchment. This study was also evidenced that the vegetation coverage of the catchment was astonishingly degraded because of the expansion of agriculture. Therefore, rehabilitation and sustainable land management system should be applied by any concerned body to restore the catchment.

5.2. Conclusion

Generally, the massive change was recorded between Agricultural land, shrub and Grassland, and forest land. It was easily shown that there was an increase of Agricultural land, built-up area, water bodies, and decrease of forested areas and shrub and grassland over 30 years in selected three times series (1989, 2002, and 2018).

Using estimated LU/LC change the SWAT model produced the required performance. The parameters were allowed to vary during the calibration and validation process within acceptable ranges across the catchment until an acceptable fit between the measured and simulated values was obtained. The SWAT model showed the required performance for both calibration and validation on the Catchment.

The effect of landuse/land cover change on streamflow in four flow periods; dry season, wet season, short rainy season, and annual and total flow daily recorders. The simulated streamflow revealed that the streamflow was increased during short rainy and wet season respectively. Whereas; the result also simultaneously showed that the streamflow decreased during the dry season due to the effect of LU/LC change. Therefore, it was very important to study on the impact of landuse/land cover on streamflow in particular attention.

5.3. Recommendations

Generally, based on the conclusion of the study, the following recommendations were made:

- ✓ LU/LC change in the Upper Guder River Catchment was mainly caused by the expansion of agricultural land. Due to this reforestation around shrub-land, steep slope land and some parts of agricultural land should be mandatory. Mainly at upstream of the catchment require more attention than other parts which is located at the middle and lower part of the catchment with other soil conservation measures.
- ✓ Due to significant LU/LC, it needs an effective integrated participatory approach for catchment management.
- ✓ The catchment was sensitive to past LU/LC change, so the government should give orientation for every stakeholder to protect the catchment by protecting their own farmland as well as the surrounding area from deforestation. Otherwise, the deforestation leads to flooding during the wet season and water scarcity during the dry season in the catchment.
- ✓ Further researches like sedimentation effects on Upper Guder River Catchment with reservoirs including detailed landuse surveys shall be done. And also catchment should have to be modeled with climate data downscaled from different scenarios.

6. REFERENCES

Abbaspour, K.C., Rouholahnejad, E., Vaghefi, S., Srinivasan, R., Yang, H. and Klove, B. (2015). A continental-scale hydrology and water quality model for Europe: Calibration and uncertainty of a high-resolution large-scale SWAT model. *Journal of Hydrology*, 524, 733–752.

Abbott, M., Bathurst, J., Cunge J.A., O'Connell, P., and Rasmussen, J. (1986). An introduction to the European Hydrologic system (SHE), Structure of a physically based distributed modelling system. *Journal of Hydrology*, 87: 61-77.

Abdo, K. S., Fiseha, B. M., & Rientjes, T. H. (2009). Assessment of climate change impacts on the hydrology of Gilgel Abay catchment in Lake Tana basin. Ethiopia. Hydrological Process. 23(26), 3661–3669.

Abebe, S. (2005). Land-Use and Land-Cover change in headstream of Abbay watershed, Blue Nile Basin. *Addis Ababa University, Ethiopia.*

ACE, U. (2001). Hydrologic Modeling System HEC- HMS User's Manual. Hydrologic Engineering Center, Davis, CA.

Aithal, B.H., Vinay, S. and Ramachandra, T.V. . (2013). Prediction of Land Use Dynamics in the Rapidly Urbanising Landscape Using Land Change Modeler. Advances in Computer Science, AETCAS, NCR, Delhi. 13-14 December 2013.

Amare, S., & Kameswara, R. (2012). Impacts of land cover/use dynamics of Gilgel Abbay catchment of Lake Tana on climate variability, Northwestern Ethiopia. Applied Geomatics,. 4,155–162.

Anderson, J., Hardy, E., Roach, J. and Witmer, R. (1976). A Land Use and Land Cover Classification System for use with Remote Sensor Data. Geological Survey Professional Paper . 964.

Arnold, J. G. (1998). Large area hydrologic modeling and assessment Part I: Model Development. *Journal of the American Water Resources Association*, 30 (1): 73-89.

Arnold, J. G. W., Moriasi, P. , J. G. Gassman, K. C. Abbaspour, M. J. White, R. Srinivasan, C. Santhi, R. D. Harmel, A. van Griensven, M. W. Van Liew, N. Kannan, & M. K. Jha. (2012). Swat: Model Use, Calibration, and Validation. Transactions of the ASABE Vol.55(4):. *American Society of Agricultural and Biological Engineers ISSN 2151-0032*, 1491-1508.

Asres M. and Awulachew S. (2010). SWAT based runoff and sediment yield modeling: A case study of Gumera Watershed in Blue Nile basin. Ecohydrology and Hydrology, Ecohydrology for water ecosystems and society in Ethiopia.

Behailu, A. (2010). Land Use and Land Cover Analysis and Modeling in South Western Ethiopia: The Case of Selected Resettlement Kebeles in GimboWoreda. *MSc Thesis, Addis Ababa University, Addis Ababa.*

Bekele, S. (2003). Challenges and opportunities in capacity building for water resources development and research in Ethiopia. Proceedings of a MOWIE/EARO/IWMI/ILRI international workshop held at ILRI, Addis Ababa, Ethiopia, 2–4 December 2002. *IWMI(International Water Management Institute), Colombo, Sri Lanka, and ILRI (International Livestock Research Institute). Nairobi, Kenya*, 141–148.

Bergstrom, S. (1995). The HBV model. In: Sing, V.P. (Ed), Computer models of watershed hydrology. *Water Resources Publications, Colorado*, 443-476.

Birhanu, A. (2014). Environmental Degradation and Management in Ethiopian Highlands: Review of Lessons Learned. *International Journal of Environmental Protection and Policy*, 2, 24-34. https://doi.org/10.11648/j.ijepp.20140201.14.

Boakye, E., Odai, S., Adjei, K., and Annor, F. (2008). Landsat images for assessment of the impact of land use and land cover changes on the Barekese Catchment in Ghana. *Eur. J. Sci. Res.*, 22 (2), 269–278.

Calder, R. (1999). The Blue Revolution. *London, Earth scan Publication ltd.*

Comenetz, J. and Caviedes, C. (2002). Climate Variability, Political Crises, and Historical Population Displacements in Ethiopia. Global Environmental Change Part B: Environmental Hazards . 4(4): 113–127 .

Congalton, R. (1991). A Review of Assessing the Accuracy of Classifications of Remotely Sensed Data. Remote Sensing of Environment. 37:35{46.).

Costa, D., Avelino, R., Sára, S., Thomazini, L., Aurélio, M. & Caiado, C. (2015). Application of the SWAT hydrologic model to a tropical watershed at Brazil. Catena. 125, 206-213. doi:10.1016/j.catena.2014.10.032.

CSA. (2015). Statistical Abstract of Ethiopia. Addis Ababa. Central Statistical Agency.

Cunderlik, M. J. (2003). *Hydrologic model selection fort the CFCAS project: Assessment of Water Resources Risk and Vulnerability to Changing Climatic Conditions.* Project Report I University of Western Ontario, Canada.

Danuso, F. (2002). A Stochastic Model for weather data generation. Italian, Journal of Agronomy.

DeFries and Eshleman. (2004). Predicting discharge at ungauged catchments : parameter estimation through the method of regionalisation.MSc-thesis. University of Twente, Enschede.

Dessie, G. and Christianson, C. (2008). Forest decline and its causes in the South-Central Rift Valley of Ethiopia: human impact over a one hundred year perspective. Ambio . 37:263-271.

Essenfelder, A. H. (2016). SWAT Weather Database:. A Quick Guide. Version: v.0.16.06. doi:10.13140/RG.2.1. 4329.1927.

FAO. (1999). Soil salinity assessment: Methods and interpretation of electrical conductivity measurements.

FAO and MoWIE . (2013). Developing a Water Audit for Awash River Basin. . *GCP/INT/072/ITA Addis Ababa, Ethiopia.*

FDRE, (Federal Democratic Republic of Ethiopia). (2004). The new coalition for food security in Ethiopia: Food Security Programme, Monitoring and Evaluation Plan (October 2004–September 2009). Addis Ababa: Food Security Coordination Bureau.

Fekadu Moreda, Victor Koren, Ziya Zhang, Seann Reed, Michael Smith. (2005). Parameterization of distributed hydrological models: learning from the experiences of lumped modeling. *Journal of Hydrology* , 320 (2006) 218–237.

Friedrich J. Koch, Ann van Griensven, Stefan Uhlenbrook, Sirak Tekleab, & Teferi, E. (2012). The Effects of Land use Change on Hydrological Responses in the Choke Mountain Range (Ethiopia) - A new Approach Addressing Land Use Dynamics in the Model SWAT UFZ – Helmholtz Centre for Environmental Research, Leipzig, Germany.

Gashaw, T., Tulu, T., & Argaw, M. (2018). Modeling the hydrological impacts of land use/land cover changes in the Andassa watershed, Blue Nile Basin, Ethiopia. Science of the Total Environment. 619–620, 1394–1408.

Gebrehiwet, K. B. (2004). Land use and land cover changes in the central highlands of Ethiopia: The case of Yerer Mountain and its surroundings. M.Sc Thesis, Addis Ababa University,.

Ginevan, M. (1979). Testing land-use map accuracy: another look. Photogrammetric another look. Photogrammetric Engineering and Remote Sensing, . 45(10):1371{1377}.

Green, W. H., and Ampt, G. A. (1911). Studies on soil physics-I. The flow of air and water through soils. *The Journal of Agricultural Science*, 4(1), 1–24 .

Hadgu, K. M. (2008). Temporal and spatial changes in land use patterns and biodiversity in relation to farm productivity at multiple scales in Tigray, Ethiopia. Wageningen University, Wageningen, The Netherlands.

Hardision, J. K. (1960). General Surface Runoff Techniques. USA: USA Government Printing office washngton.

Haregeweyn, N., Tsunekawa, A., Nyssen, J., Poesen, J., Tsubo, M., Tsegaye Meshesha, D., Schütt, B., Adgo, E., Tegegne, F. (2015). Soil erosion and conservation in Ethiopia: a review. Prog. Phys. Geogr. 39 (6), 750–774.

Haron, S. H., Khalid, K., Ali, M. F., Faiza, N. and Rahman, A. (2016). Application of the SWAT Hydrologic Model in Malaysia : Recent Research Application of the SWAT Hydrologic Model in Malaysia :, (March).

Hurni, H., Kebede, T. and Zeleke, G. (2005). The Implications of Changes in Population, Land Use, and Land Management for Surface Runoff in the Upper Nile Basin Area of Ethiopia. *Mountain Research and Development*, 25(2): pp. 147–154.

IGBP-IHDP. (1999). *International Geo-Sphere Biosphere Program and The International Human Dimension Program, Land-use and land-cover change, implementation strategy. IGBP Report 46/IHDP Report 10.* Stockholm and Bonn.: Prepared by Scientific Steering Committee and International Project Office of LUCC.

J. A. Velazquez´, F. Anctil , and C. Perrin. (2010). Performance and reliability of multimodel hydrological ensemble simulations based on seventeen lumped models and a thousand catchments. *Hydrol. Earth Syst. Sci.*, 14, 2303–2317, 2010.

James, L. D., & Burges, S. (1982). Selection, calibration, and testing of hydrologic models. In H. J. C. T. Haan & J. A. Basselman (Eds.), Hydrologic modeling of small watersheds, ASAE Monograph . (pp. 437–472). St. Joseph, MI: American Society of Agricultural Engineers.

Jha, M. K. (2011). Evaluating Hydrologic Response of an Agricultural Watershed for Watershed Analysis. 604-617. doi:10.3390/w3020604.

Jiang, S., Ren, L., Yomg, B., Singh, V.P., Yang, X., and Yuan, F. (2011). Quantifying the effects of climate variability and human activities on runoff from the Laohahe basin in northern China using three different methods. Hydrological Processes. doi: 10.1002/hyp.8002.

Julien, P. Y. (2010). Erosion and Sedimentation. Cambridge: United States of America by Cambridge University Press, New York.

Kaimowitz, D. and Angelsen, A. (1998). Economic Models of Tropical Deforestation Review by the Center for International Forestry Research. (In Indonesia).

Kassa, T. (2009). Watershed Hydrological Responses to Changes in Land Use and Land Cover, and Management Practices at Hare Watershed, Ethiopia. PhD Dissertation, University.

Khatun, S. (2018). Simulation of surface runoff using semi distributed hydrological model for a Simulation of surface runof using semi distributed hydrological model for a part of Satluj

Basin : parameterization and global sensitivity analysis using SWAT CUP. . *Modeling Earth Systems and Environment,*, 0(0), 0. doi:10.1007/s40808–018–0474–5.

Kidane M, Terefe T, Bezie A, Kessete N, and Endrias M. (2018). Evaluating the impacts of climate and land use/land cover (LU/LC) dynamics on the Hydrological Responses of the Upper Blue Nile in the Central Highlands of Ethiopia,. *Spatial Information ResearchAmbo University, Ethiopia, DOI 10.1007/s41324-018-0222-y* , 18-19p.

Kumar, S.K., Valasala, S., Subrahmanyam, V.J., Mallampati, M., Shaik, K. and Ekkirala. (2015). Prediction of Future Land-Use Land-Cover Changes of Vijayawad City Using Remote Sensing and GIS. International Journal of Innovative Research in Advanced Engineering. 2, 91-97.

Lambin E. F., Rounsevell, M. D. A and Geist, H. J. (2000). Are agricultural land-use models able to predict changes in land-use intensity? Agriculture, Ecosystems and Environment. 82, 321-331.

Lambin, E. F. (2003). Dynamics of land use and land cover change in tropical regions. *Annu. Rev. Environ. Resource.*, 28: 205- 41.

Ma X, X. (2009). Responses of hydrological processes to land-cover and climate changes in Kejie watershed,. south-west China. Hydrological Processes . 23, 1179-1191.

Matjaz, G. and Marina, P. (2012). Strengths, Weaknesses, Opportunities and Threats of Catchment Modelling with Soil and Water Assessment Tool (SWAT) Model. *Journal of researchGate*, 60-61.

McColl, C. (2007). Improved land use decision support, land use forecasting and hydrologic model Integration, RGIS Pacific Northwest. Central Washington University.

Mengistie, K., S., Demel, T., and Knoke, T. (2013). Land Use/Land Cover Change Analysis Using Object-Based Classification Approach in Munessa-Shashemene Landscape of the Ethiopian Highlands. *Journal of Remote Sensing*, 5, 2411-2435. https://doi.org/10.3390/rs5052411.

Meyer, W.B. and Turner, B. L. (1994). Changes in Land Use and Land Cover: A Global Perspective. *Cambridge, Cambridge University Press, New York.*

Minichil, J. (2016). Evaluation of land use land cover change on Stream flow. a case study of dedissa sub basin, abay basin, south western Ethiopia,Ariba Minch University.

Miranda, J. D., Armas, C., Padilla, F. M. and Pugnaire, F. I. (2011). Climatic Change and Rainfall Patterns: Effects on Semi-Arid Plant Communities of the Iberian Southeast. *Journal of Arid Environments*, 75(12): pp1302–1309. .

Mishra, V.N., Rai, P.K. and Mohan, K. (2014). Prediction of Land Use Changes Based on Land Change Modeler Using Remote Sensing: A Case Study of Muzaffarpur (Bihar), India. . *Journal of the Geographical Institute "Jovan Cvijic" SASA,* , 64, 111-127. https://doi.org/10.2298/IJGI1401111M.

Monserud, R. A. (2003). Evaluating forest models in a SFM context. Forest Biometry, Modelling and Information Sciences . 1(1). Pp. 35-47.

Montoya, J. M. and Raffaelli, D. (2010). Climate Change, Biotic Interactions and Ecosystem Services. . *Phil. Trans. R. Soc. B.*, 365(1549): pp. 2013–2018.

Moriasi, D., Arnold, J., and Liew, M. W. (2013). *Model Evaluation Guidelines for Systematic Quantification of Accuracy in Watershed Simulations. doi:10.13031/2013.23153.*

Moriasi, N. D. (2007). Model Evaluation Guidelines for Systematic Quantification of Accuracy in Watershed Simulations. American Society of Agricultural and Biological Engineers.

Mwangi, H. M., Julich, S., & Patil, S. D. (2016). Relative contribution of land use change and climate variability on discharge of upper Mara River, Kenya. *Journal of Hydrology: Regional Studies*, 5, 244–260.

Neitsch, S. A. (2005). Soil and Water Assessment Tool, Theoretical documentation: Version 2005. *Temple, TX.USDA Agricultural Research Service and Texas A & M Black land Research Centre*.

Neitsch, S.L., Arnold, J.R., and Kiniry, J.R. (2005). Soil and Water Assessment Tool (SWAT) Input/output File Documentation, Version 2005, Grassland Soil and Water Research Laboratory. *Agricultural Research Service, Blackland Research Center, Texas Agricultural Experiment station*.

Oumer, H. A. (2009). Land Use And Land Cover Change,Drivers And Its Impact: A Comparative Study From Kuhar Michael And Lenche Dima Of Blue Nile And AwashBasins Of Ethiopia. Corrnell University.

Panhalkar, S. S. (2014). Hydrological modeling using SWAT model and geoinformatic techniques. . *the egyptian journal of remote sensing and space*., doi:10.1016/j.ejrs.2014.03.001.

Polanco, E. I., Fleifl, A., Ludwig, R. & Disse, M. (2017). Improving SWAT model performance in the upper Blue Nile Basin using meteorological data integration and subcatchment discretization,. 4907-4926.

Pontius, R.G. and Chen, H. (2006). GEOMOD Modelling, Land-Use & Cover Change Modelling. Clark University, Worcester.

Rabo, G. (2018). Simulation of Runoff under the past impacts of land use land cover and future climate change (Case Study of Anger sub basin). *Master of thesis. Addis Ababa University, Ethiopia*, 49,50p.

Refsgaard, J. C. (1996). Parameterisation, calibration and validation of distributed hydrological models. *Journal of Hydrology* , 198 (1997) 69–97.

Richards, H. M. (1998). Hydrologic Analysis and Design. Department of Civil Engineering University of Maryland, Prentice Hall Upper Saddle River. *New Jersey 074582ndEdition.*

Rientjes, T.H.M., Haile, A.T., Kebede, E., Mannaerts, C.M.M., Habib, E., and Steenhuis, T.S. (2011b). Changes in land cover, rainfall and stream flow in Gilgel Abbay catchment, Upper Blue Nile basin–Ethiopia. . *Hydrol. Earth Syst. Sci.*, 15, 1979–1989, 2011, doi: 10.5194/hess-.

Rosenfield, G. (1982). Analysis of variance of thematic mapping experiment data. Photogrammetric Engineering and Remote Sensing. 47(12):1685{1692.

Sage, C. (1994). Population and Income. In Meyer, W.B. and Turner, B. L. Change in land use and land cover. *A Global perspective Cambridge university press: Cambridge*, 263- 285 pp.

Santhi, C. J. (2001). Validation of the SWAT model on a large river basin with point and non point sources the American water resources association. 1169-1188.

Scott, N. M., William, G. K., & Megan, H. M. (2002). Integrating Landscape Assessment and Hydrologic Model for Land Cover Change Analysis. *Journal of the American Water Resources Association*, 28(4), 915–929.

SCS, U. (1972). *National Engineering Handbook, Section 4: Hydrology*. Washington, DC: U.S. Government Printing Office.

Setegn, S. S. (2008). Spatial delination of soil erosion vulnerability in the Lake Tana Basin, Ethiopia. Hydrological Processes, Hydrol. Process. (2009).

Sherbinin, D. (2002). Predicting discharge at ungaugedcatchments : parameter estimation through the method of regionalisation.MSc-thesis.University of Twente, Enschede.

Sith, R. & Nadaoka, K. (2017). Comparison of SWAT and GSSHA for High Time Resolution Prediction of Stream Flow and Sediment Concentration in a Small Agricultural Watershed. *Hydrology*, 4(2), 27. doi:10.3390/hydrology4020027.

Solomon, G., Trier, G., Woldeamlak, B., Gardenas, A., and Bishop, K. (2014). Forest cover change over four decades in the Blue Nile Basin, Ethiopia: comparison of three watersheds. *Reg. Environ. Change* , 14, 253–266.

Solomon, H. (2005). GIS-Based Surface Runoff Modeling and Analysis of Contributing Factors; a Case study of the Nam Chun watershed. *Thailand. M.Sc Thesis, ITC, the Netherlands.*

Tadesse, T. (2016). Development of Water Allocation and Utilization System for Koka Reservoir under Climate Change and Irrigation Development Scenarios (Case Study Downstream of Koka Dam to Metahara). Addis Ababa Ethiopia. 28.

Teferi, E., Uhlenbrook, S., Bewket, W., Wenninger, J., and Simane, B. (2010). The use of remote sensing to quantify wetland loss in the Choke Mountain range, Upper Blue Nile basin, Ethiopia. *Hydrol. Earth Syst. Sci.* , 14, 2415–2428.

Tekle, A. (2010). Assessment of Climate change impact on Water availability of Bilate watershed, Ethiopian Rift valley basin. M.Sc Thesis, Arba Minch University, Ethiopia.

Temesgen, G., Amare, B., and Abraham, M. (2014). Evaluations of land use/land cover changes and land degradation in Dera District, Ethiopia: GIS and remote sensing based analysis. *Int. J. Sci. Res. Environ. Sci.*, 2 (6), 199–208.

Tolba, M.K., and El-Kholy, O.A. (1992). The World Environment 1972–1992: Two Decades of Challenge, Chapman & Hall, London.

Tolessa, T., Senbeta, F., & Kidane, M. (2016). Landscape composition and configuration in the central highlands of Ethiopia. Ecology and Evolution. 6, 7409–7421.

Tracy, J. B., Scott, N. M., & Kenneth, L. D. (2007). Assessing land cover change in Kenya's Mau Forest region using remotely sensed data. African Journal of Ecology. 46(1), 46–54.

Tuppad, P., Mankin, K. R. D., Lee, T., Srinivasan, R. & Arnold, J. G. (2011). soil and water assessment tool (swat) hydrologic/water quality model: extended capability and wider adoption. *American Society of Agricultural and Biological Engineers*, ISSN 2151–0032, 54(2007), 1677-1684.

Turner, B. L., Moss, R. H., & Skole, D. L. (1993). Relating land use and global land cover change: A proposal for an IGBP-HDP core project. Stockholm: International Geosphere-Biosphere Programme: A Study of Global Change and the Human Dimensions of Global Environmental Change Programme.

Uttam Ghimire, Anshul Agarwal, Narayan Kumar Shrestha, Prasad Daggupati, Govindarajalu Srinivasan, and Htay Htay Than . (2020). Applicability of Lumped Hydrological Models in a Data-Constrained River Basi n of Asia. *ASCE, ISSN 1084-0699*, 10.1061/(ASCE)HE.1943-5584.0001950.

Van Griensven, A. M. (2006). A global sensitivity analysis tool for the parameters of multivariable catchment models . *Journal of Hydrology*, 324: 10-23p.

Wang, G.X., Liu, J.Q., Kubota, J., and Chen, L. (2007b). Effect of land-use changes on hydrological processes in the middle basin of the Heihe River, northwest China. . *Hydrological Processes* , 21:1370–1382, doi: 10.1002/hyp.6308.

Welde, K., & Gebremariam, B. (2017). Effect of land use land cover dynamics on hydrological response of watershed: Case study of Tekeze Dam watershed, northern Ethiopia. . *International Soil and Water Conservation Research*, 5, 1–16.

Williams, J. (1981). Testing the modified Universal Soil Loss Equation, in Estimating Erosion and Sedinzent Yield on Rangelands, USDA. ARM-W-26: 157-1 64 .

Yang, Z., Zhou, Y., Wenninger, J., and Uhlenbrook, S. (2012). The cause of flow regime shift in the semi- arid Humiliate River Northwest China. *Hydrology and. Earth System Science*, 16: 87–103, doi: 10.5194/hess-16-87.

Zeleke, G. A. (2001). Implications of Land use and land cover dynamics for mountain resource degradation in the northwestern Ethiopia. highlands Mountain Research and Development. 21: 184-191.

Zhan, J., Liu, J., Lin, Y., Feng, W.Y. and Ma, E. . (2014). Chapter 2, Land Use Change Dynamics Model Compatible with Climate Models. https://doi.org/10.1007/978-3-642-54876-5_2.

7. APPENDICES

7.1. Appendix Tables

Appendix Table 1: Annual rainfall stations used in developing double mass curve

Year	Tikur Enchini	Ambo	Guder	Gedo
1989	1926.53	1049.93	1188.90	1203.90
1990	2115.10	1117.80	1601.30	839.60
1991	1356.90	1271.43	1652.50	917.08
1992	1542.90	1685.85	2402.10	1127.63
1993	2465.70	1157.80	2650.10	1066.78
1994	1294.20	1334.55	1758.00	913.45
1995	1722.95	1235.01	1280.70	710.57
1996	2321.70	1646.17	2045.30	571.50
1997	1753.20	871.87	1799.00	726.30
1998	1925.20	1203.27	1060.50	699.20
1999	1598.40	821.60	1321.80	568.13
2000	1643.00	904.10	1439.00	682.77
2001	1968.30	1079.50	1391.50	1542.90
2002	1810.10	813.86	961.50	831.70
2003	1747.00	932.20	1332.20	848.00
2004	1837.30	944.00	1488.20	650.90
2005	1734.20	856.60	1379.50	811.70
2006	1979.70	1128.73	1501.30	1343.60
2007	1785.20	1163.10	1345.90	1062.50
2008	1901.70	1160.30	1184.00	1346.80
2009	1635.13	1006.40	1278.00	764.80
2010	2002.60	1187.60	1150.60	992.60
2011	1830.40	1885.10	1185.50	612.60
2012	1551.90	956.10	859.50	830.80
2013	2114.00	960.00	1073.70	912.80
2014	2045.83	866.10	759.40	873.30
2015	1818.70	895.77	1045.00	891.70
2016	1901.80	1091.13	1652.40	1014.30
2017	1766.80	830.97	820.40	1255.00
2018	1828.91	985.66	1047.87	1341.70

Appendix Table 2: Mean monthly flow of Guder streamflow (m^3/s)

Year	Jan	Feb	Mar	Apr	May	Jun	Jul	Aug	Sep	Oct	Nov	Dec
1995	0.62	0.53	0.48	1.01	1.45	3.10	20.33	44.22	29.32	4.18	1.21	0.86
1996	0.92	0.55	2.45	2.16	6.74	29.46	39.48	45.81	26.50	9.74	2.04	1.08
1997	1.05	0.65	0.71	1.54	1.32	10.90	36.05	37.03	18.29	8.77	3.74	2.20
1998	1.35	0.77	1.29	0.62	0.98	6.98	32.70	45.44	33.39	22.55	3.11	1.06
1999	0.80	0.45	0.47	0.33	1.47	10.88	33.20	44.46	32.53	23.48	3.15	1.40
2000	0.97	0.67	0.56	1.43	2.10	9.58	21.44	41.20	46.16	21.51	6.03	1.16
2001	1.20	0.83	2.42	1.90	3.25	27.99	41.07	37.11	31.11	11.98	2.48	1.21
2002	1.11	0.76	0.79	1.28	1.72	6.31	34.79	34.50	22.11	4.08	1.20	0.98
2003	0.89	0.70	1.32	1.54	0.67	3.79	30.19	41.05	34.26	7.81	1.49	1.07
2004	0.86	0.63	0.68	1.42	1.09	4.87	24.59	37.08	35.32	16.29	1.48	0.84
2005	0.72	0.32	0.72	1.09	2.19	7.45	30.11	39.36	29.01	10.91	1.78	0.70
2006	0.49	0.34	1.55	1.92	1.54	13.28	39.24	74.08	39.79	9.64	2.00	1.27
2007	0.84	0.89	0.64	0.69	2.88	13.72	43.09	47.52	55.31	11.95	1.18	0.67
2008	0.49	0.45	0.33	0.48	2.32	25.04	56.58	51.24	55.03	4.32	10.01	1.01
2009	0.83	0.73	0.32	0.85	0.62	1.58	24.74	51.14	26.66	10.12	3.05	1.93

Appendix Table 3: Sensitivity rank for daily calibration

No	Parameter Name	t-Stat	P-Value	sensitivity rank
1	5:R__OV_N.hru	43.022	0.000	1
2	2:V__GW_DELAY.gw	-3.161	0.002	2
3	9:R__SFTMP.bsn	-2.264	0.024	3
4	7:R__SOL_AWC (...).sol	1.557	0.032	4
5	3:R__ESCO.bsn	-1.288	0.038	5
6	11:R__SOL_BD (...).sol	-0.803	0.042	6
7	1:R__CN2.mgt	0.730	0.466	7
8	6:R__CH_N2.rte	0.728	0.467	8
9	12:R__GW_REVAP.gw	-0.587	0.558	9
10	4:R__SLSUBBSN.hru	0.275	0.783	10
11	8:R__ALPHA_BNK.rte	-0.242	0.809	11
12	10:R__SURLAG.bsn	0.216	0.829	12

Note: “V_” indicates replacement by a new value; “R_” indicates relative change; suffixes rte, sol, gw etc are SWAT file extensions.

7.2. Appendix Figures

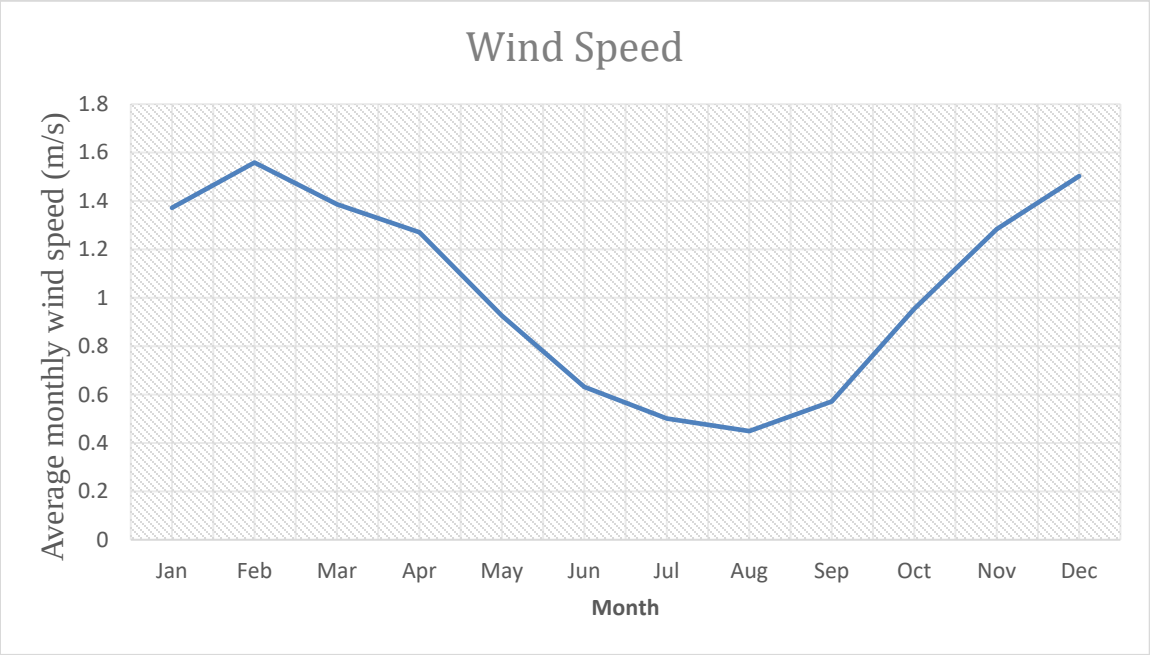

Appendix Figure 1: Average monthly graph of wind speed (1989-2018)

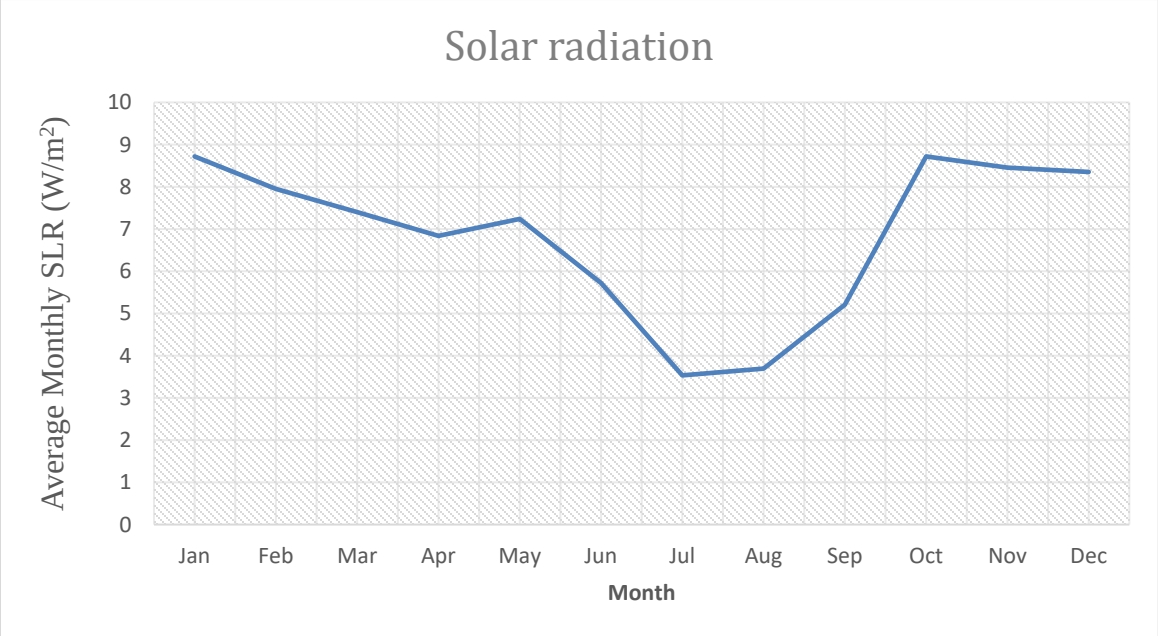

Appendix Figure 2: Average monthly graph of solar radiation (1989-2018)

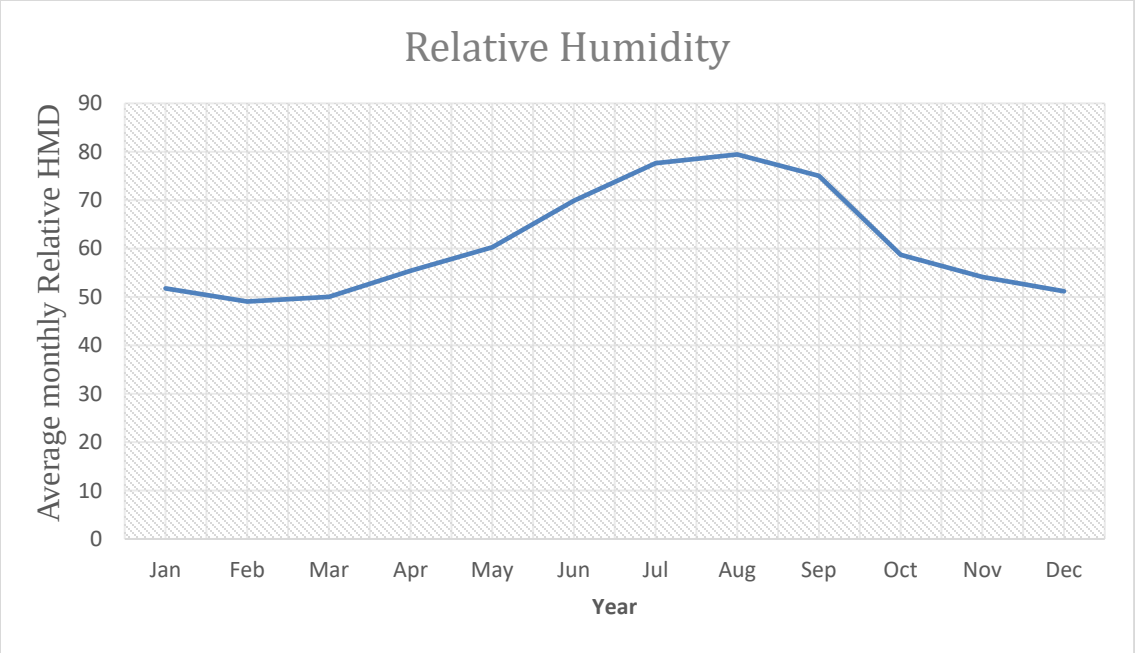

Appendix Figure 3: Average monthly graph of relative humidity (1989-2018)

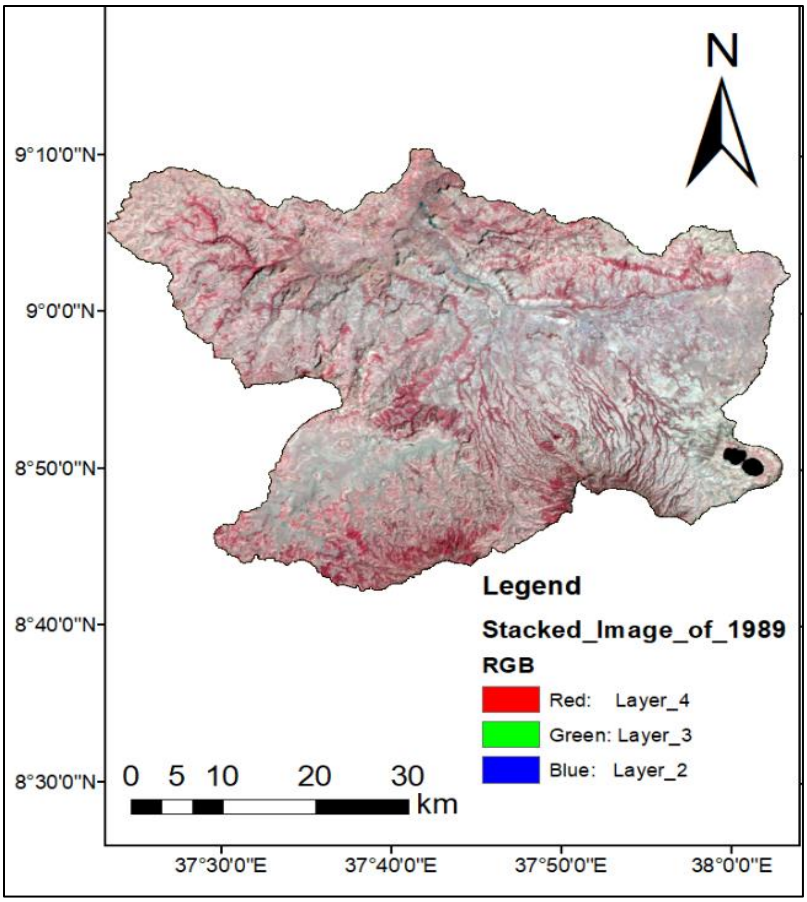

Appendix Figure 4: "False color" composite satellite image of the study area during 1989

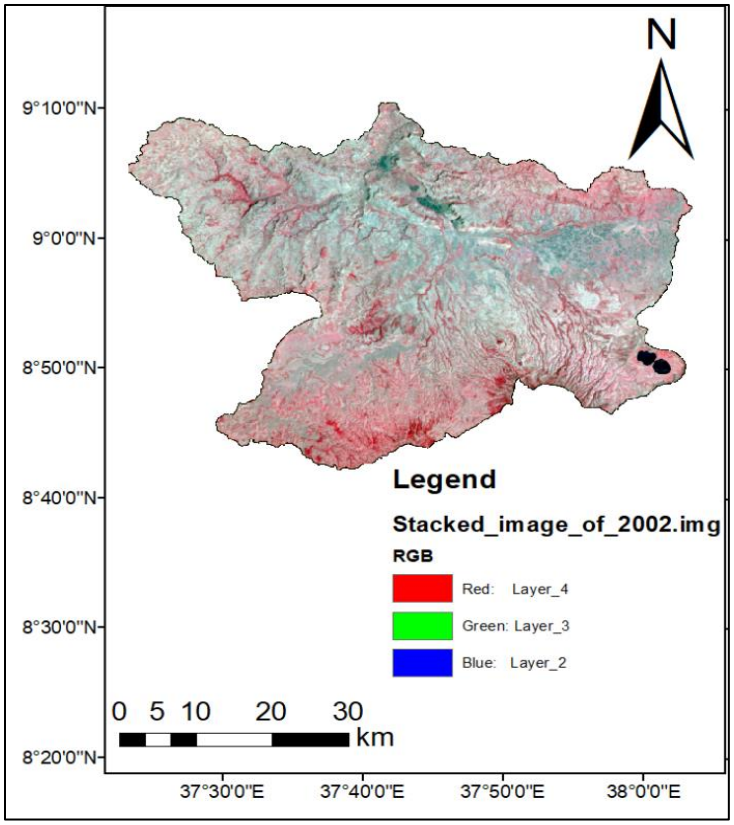

Appendix Figure 5: “False color" composite satellite image of the study area during 2002

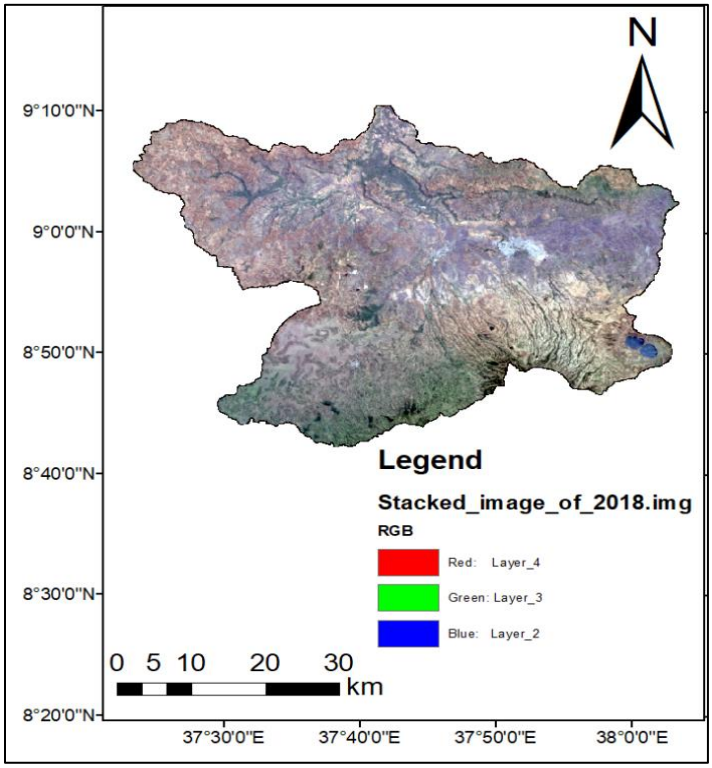

Appendix Figure 6: “False color" composite satellite image of the study area during 2018

(a)

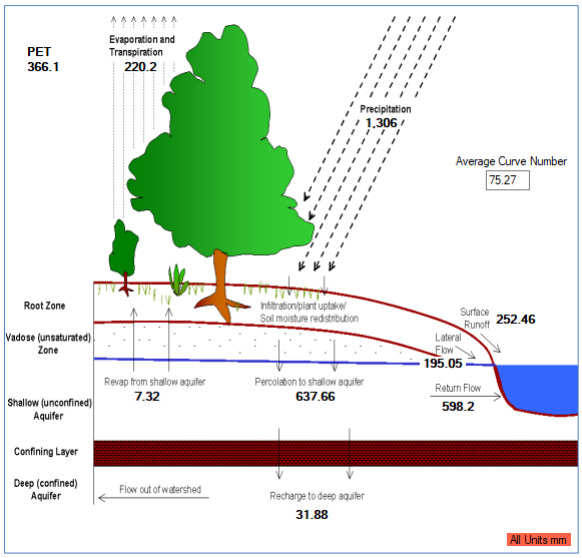

(b)

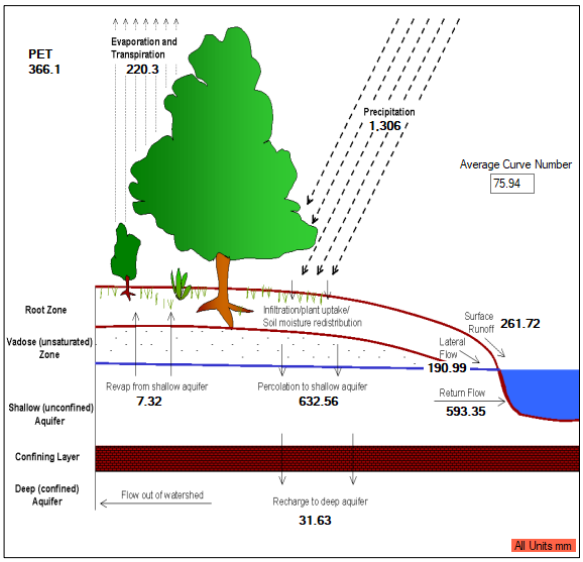

(c)

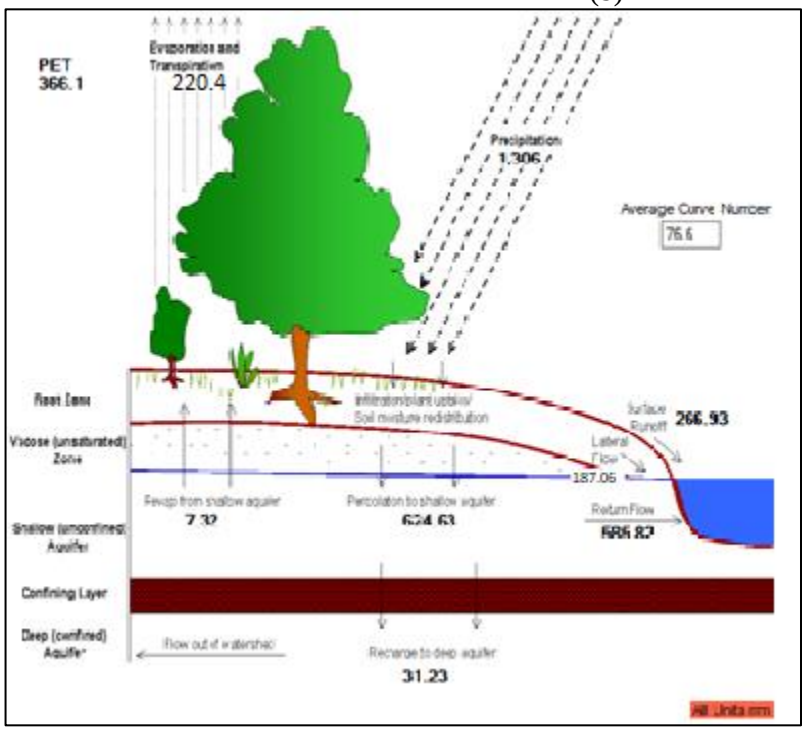

Appendix Figure 7:: The realistic difference in hydrology of catchment due to (a) 1989 LU/LC, (b) 2002 LU/LC, and (c) 2018 LU/LC.